JCI The Journal of Clinical Investigation

Filgotinib suppresses HIV-1-driven gene transcription by inhibiting HIV-1 splicing and T cell activation

Yang-Hui Jimmy Yeh, … , Steven G. Deeks, Ya-Chi Ho

J Clin Invest. 2020. https://doi.org/10.1172/JCI137371.

Research In-Press Preview AIDS/HIV Therapeutics

Graphical abstract

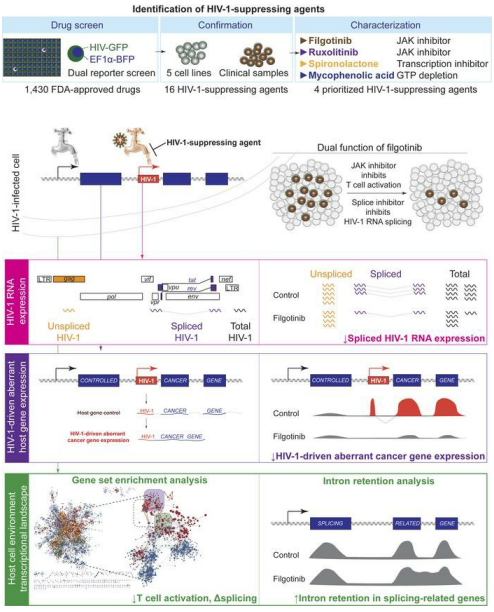

Find the latest version:

https://jci.me/137371/pdf

Filgotinib suppresses HIV-1-driven gene transcription by inhibiting HIV-1 splicing and T cell activation

Authors: Yang-Hui Jimmy Yeh[1], Katharine M. Jenike[2], Rachela M. Calvi[3], Jennifer Chiarella[3], Rebecca Hoh[4], Steven G. Deeks[4], Ya-Chi Ho[1]*

Affiliations:

[1]Department of Microbial Pathogenesis, Yale University School of Medicine, New Haven, CT 06519, USA

[2]Human Genetics PhD Program, Johns Hopkins University School of Medicine, Baltimore, MD 21205, USA

[3]Department of Neurology, Yale University School of Medicine, New Haven, CT 06519, USA

[4]Department of Medicine, University of California, San Francisco, CA 94110, USA

*Address correspondence to:

Ya-Chi Ho

Department of Microbial Pathogenesis, Yale University School of Medicine, 295 Congress Ave, New Haven, CT 06519, USA

Phone: 203-785-4052

Email: ya-chi.ho@yale.edu

Conflict of interest statement:

Y.-C.H. receives research grants from Gilead Sciences awarded to Yale University and there is no competing interest. The rest of the authors have declared that no conflict of interest exists.

Abstract: Despite effective antiretroviral therapy, HIV-1-nfected cells continue to produce viral antigens and induce chronic immune exhaustion. We propose to identify HIV-1-suppressing agents which can inhibit HIV-1 reactivation and reduce HIV-1-induced immune activation. Using a novel dual reporter system and a high-throughput drug screen, we identified FDA-approved drugs which can suppress HIV-1 reactivation in both cell line models and $CD4^+$ T cells from virally suppressed, HIV-1-infected individuals. We identified 11 cellular pathways required for HIV-1 reactivation as druggable targets. Using differential expression analysis, gene set enrichment analysis and exon-intron landscape analysis, we examined the impact of drug treatment on the cellular environment at a genome-wide level. We identified a new function of a JAK inhibitor filgotinib which suppresses HIV-1 splicing. First, filgotinib preferentially suppresses spliced HIV-1 RNA transcription. Second, filgotinib suppresses HIV-1-driven aberrant cancer-related gene expression at the integration site. Third, we found that filgotinib suppresses HIV-1 transcription by inhibiting T cell activation and by modulating RNA splicing. Finally, we found that filgotinib treatment reduces the proliferation of HIV-1-infected cells. Overall, the combination of a drug screen and transcriptome analysis provides systemic understanding of cellular targets required for HIV-1 reactivation and drug candidates that may reduce HIV-1-related immune activation.

Introduction

Despite effective antiretroviral therapy (ART), HIV-1 persists in the latent reservoir which is a major barrier to cure (1-3). Treatment interruptions lead to viral rebound from latently infected cells (4). One of the strategies to curing HIV-1 infection is the shock-and-kill strategy, which reverses HIV-1 latency and exposes HIV-1-infected cells for immune clearance (5, 6). To prevent systemic toxicity, an ideal latency reversing agent should reverse HIV-1 latency without causing global T cell activation. Extensive small molecule compound library screens have identified latency reversing agents, such as histone deacetylase inhibitors, protein kinase C agonists, non-canonical NF-κB activators, which can reactivate HIV-1 in vivo (5, 7-10). Yet, while latency reversing agents can induce HIV-1 RNA transcription, recent evidence suggests that latency reversal without T cell activation is not sufficient to induce antigen presentation and immune clearance (11, 12). Understanding the cellular environment supporting HIV-1 transcription is required to develop effective HIV-1 eradication strategies.

Latent HIV-1 proviruses in quiescent memory $CD4^+$ T cells are largely transcriptionally inactive. This is because of the lack of active transcription factors and the Tat positive feedback loop (13-17), transcriptional blocks (18) and the repressive chromatin environment (19-22). Upon antigen stimulation, T cell receptor signaling leads to AP-1 (23), NFAT (24) and NF-κB (25) transcription factor activation, nuclear translocation, binding to the HIV-1 promoter, and induces robust HIV-1 reactivation. Even without latency reversing agents, stochastic antigen stimulations in vivo reactivate HIV-1 from latency at ~0.4 events per day (26, 27). This is evidenced by the fact that HIV-1 RNA expression can be readily detected in $CD4^+$ T cells from ART-treated, virally suppressed HIV-1-infected individuals in the absence of ex vivo latency reversal (28, 29). Therefore, despite effective ART, chronic HIV-1 antigen production leads to chronic immune activation (28, 30-33), immune exhaustion (34), the residual immune dysregulatory syndrome (35, 36), premature atherosclerosis (37, 38) and accelerated aging (39, 40). Before a safe, scalable, affordable, and generalizable HIV-1 eradication strategy is

available, HIV-1-infected individuals continue to suffer from chronic immune activation (41). To halt HIV-induced immune dysfunction and chronic immune activation, therapeutic strategies which can inhibit HIV-1 transcription are required.

ART inhibits viral enzyme function or viral entry but does not inhibit HIV-1 transcription and viral antigen production. While immune modulatory strategies can enhance immune effector functions, stopping antigen production from HIV-1-infected cells is the key to block HIV-1-induced immune dysfunction. To target HIV-1 transcription effectively, a comprehensive understanding of cellular pathways both sufficient and necessary for HIV-1 transcription is needed. HIV-1 latency reversing agents searching such as drug screens (5, 42) and cellular factor screens (43, 44) identified drugs or cellular pathways *sufficient* for HIV-1 reactivation, but not necessarily identifies those *required* for HIV-1 transcription. Drug and cellular factor screens searching for agents which can suppress HIV-1 transcription would identify cellular pathways required for HIV-1 transcription, such as Tat transactivation, mTOR signaling, cation transport and estrogen receptor signaling (45-49). However, while these HIV-1-suppressing agents were reported individually, a full picture of targetable cellular pathways necessary for HIV-1 transcription remains unclear to the field.

Here we combined a novel dual reporter high-throughput drug screen system and three genome-wide transcriptome analysis approaches to systemically identify drugs and cellular pathways that can inhibit HIV-1 transcription after the establishment of latency. We confirmed that the androgen antagonist and a modest diuretics spironolactone (50), a guanosine triphosphate (GTP) depleting agent mycophenolic acid (51), and a Janus kinase (JAK) inhibitor ruxolitinib (52) can suppress HIV-1 transcription as previously reported. We identified a new JAK inhibitor filgotinib which can inhibit HIV-1-driven aberrant host gene expression in addition to inhibiting HIV-1 transcription. Filgotinib is an immune modulatory agent widely used in autoimmune diseases such as rheumatoid arthritis (53), ankylosing spondylitis (54), psoriatic arthritis (55), and Crohn's disease (56). Our goal is both

to probe for cellular pathways required for HIV-1 transcription and to identify drugs which can suppress HIV-1 transcription.

Results

A dual reporter screen identified FDA-approved drugs which can preferentially inhibit HIV-1 transcription as HIV-1-suppressing agents

To identify drugs which can preferentially inhibit HIV-1 expression, we developed a dual reporter HIV-1-infected Jurkat T cell system. These dual reporter HIV-1-infected Jurkat T cell clones harbor both HIV-1-green fluorescent protein (HIV-1-dsGFP) reporter (42) and EF1α-driven blue fluorescent protein (EF1α-dsBFP) lentiviral reporter (Figure S1A). HIV-1-dsGFP reports HIV-1 expression levels while EF1α-dsBFP serves as a counter-screen to measure drug effects on host gene transcription. Decreased HIV-1-dsGFP expression with minimal changes in EF1α-dsBFP expression indicates preferential suppression of HIV-1 expression over the host gene expression. Both dsGFP and dsBFP are destabilized (ds) through PEST sequence-mediated ubiquitination, leading to a short half-life of two hours (42) and a real-time reflection of HIV-1-dsGFP and EF1α-dsBFP expression levels. We targeted HIV-1-dsGFP to endoplasmic reticulum through the signal peptide and targeted EF1α-dsBFP to the nucleus through a nuclear localization signal to prevent fluorescence resonance energy transfer (FRET) between BFP and GFP. Different from J-Lat T cell lines which have low to no HIV-1 transcription at baseline, we identified clones which have high basal levels (>40%) of HIV-1 transcription, namely 1B6-du, 5F9-du, and 6C6-du. This strategy provides a wide dynamic range of HIV-1-dsGFP expression and allows us to identify drugs which can suppress HIV-1 expression. Further, we identified clones in which HIV-1 reporters were integrated into introns of actively transcribed genes to recapitulate HIV-1-integration into introns of actively transcribed genes observed in HIV-1-infected individuals (57, 58). Overall, our novel dual reporter HIV-1-infected Jurkat T cell system allow real-time detection of HIV-1 transcription states, a counter-screen reflecting cellular gene transcription state, and integration into introns recapitulating HIV-1-integration patterns observed in vivo.

The landscape of cellular pathways required for HIV-1 transcription as druggable therapeutic targets

We used an FDA-approved small molecule compound library to identify HIV-1-suppressing agents. While this library does not contain epigenetic silencing agents, the use of FDA-approved drugs identifies agents with known clinical toxicity profiles and allows for efficient clinical application. Drugs which suppress HIV-1-dsGFP expression below three standard deviations from mean with EF1α-dsBFP expression in 1B6-du clone were defined as candidate HIV-1-supressing agents (Figure S1B, Figure 1A). From 1,430 FDA-approved small molecule drugs, we identified 11 cellular pathways and 16 putative HIV-1-suppressing agents (Table S1, Figure 1A, Figure 2) that inhibit HIV-1 transcription. Our screen is confirmed previously reported agents which can inhibit HIV-1 transcription, such as JAK inhibitor ruxolitinib (59), DNA helicase inhibitor spironolactone (50), GTP synthesis inhibitor mycophenolic acid (51), transcription inhibitor flavopiridol (60), cation transporter inhibitors levosimendan (45) and digoxin (46). Consistent with previous findings (61), mTOR inhibitors do not significantly suppress HIV-1 transcription in our model. We also identified FDA-approved drugs which can target pathways known to affect HIV-1 transcription, such as uprosertib for Akt inhibition (62) and KPT-330 for CRM1-mediated nuclear RNA export (63). Importantly, we identified drugs and cellular pathways which were not previously known to affect HIV-1 transcription, such as dovitinib, pazopanib and ponatinib which inhibit receptor tyrosine kinase pathways and mitomycin C, irinotecan and mitoxantrone which inhibit DNA unwinding (Table S1, Figure 2).

Because one cell line model may not recapitulate the heterogeneous HIV-1 integration sites in vivo, we tested the effect of these 16 HIV-1-suppressing agents in two additional cell line clones and in $CD4^+$ T cells from virally suppressed HIV-1-infected individuals (Table S2). We first examined dose-response curves and cellular viability using flow cytometry in the two additional cell line clones 5F9-du and 6C6-du (Figure S1C, Figure S2). These cell line clones

harbor HIV-1-dsGFP proviral reporters integrated into introns of different host genes (Figure S2). We found that eight drugs (filgotinib, digoxin, levosimendan, zinc pyrithione, irinotecan, mitomycin C, mycophenolic acid, and spironolactone) suppress HIV-1-dsGFP expression without affecting EF1α-dsBFP expression and cellular viability in both of the additional cell lines (Figure S2).

JAK1 inhibitor Filgotinib is a novel HIV-1-suppressing agent

Considering the feasibility for systemic dosing and clinical adverse effects, we focused on JAK inhibitors filgotinib, a new generation JAK1 inhibitor which has not been reported to affect HIV-1 transcription. We used ruxolitinib, a JAK inhibitor known to suppress HIV-1 transcription (52)(NCT02475655) to compare whether filgotinib-mediated HIV-1 suppression is the same or different from other JAK inhibitors. To examine whether filgotinib suppresses HIV-1 transcription through distinct mechanisms, we used two drugs known to suppress HIV-1 transcription (the DNA helicase inhibitor spironolactone (50) and IMPDH inhibitor mycophenolic acid (51, 64)(NCT03262441)) as positive controls. These four drugs (filgotinib, ruxolitinib, spironolactone and mycophenolic acid) have minimal suppression of EF1α-dsBFP expression (< 0.5 standard deviation from mean) and minimum cytotoxicity (>80% cellular viability)(Figure S2).

We first examined the dose response curves using additional three cell line clones 8B10 (harboring HIV-1-dsGFP integrated into *VAV1*), 1G2 (harboring HIV-1-dsGFP integrated into *RAP1B*), and 1D7 (harboring HIV-1-dsGFP integrated into *SPECC1*) (Figure 1B). Filgotinib and spironolactone remarkably suppresses HIV-1-dsGFP expression (-61% and -74%, respectively). The 50% maximum inhibitory concentration (IC50) of filgotinib and spironolactone (~7 μM and 4 μM, respectively) is within 3 fold of the plasma levels observed in clinical use (3.4 μM (65) and 1.5 μM (66), respectively). Ruxolitinib and mycophenolic acid minimally suppresses HIV-1-dsGFP expression (0% and 50%, respectively) in these three cell lines.

We next examined the effect of these four HIV-1-suppressing agents on $CD4^+$ T cells from virally suppressed, HIV-1-infected individuals. We treated $CD4^+$ T cells from virally suppressed HIV-1-infected individuals (Table S2) with HIV-1-suppressing agents for 24 hours and stimulated these cells with phorbol myristate acetate (PMA) and ionomycin during the final 6 hours to test whether cells treated with HIV-1-suppressing agents can resist PMA/ionomycin-induced maximum latency reversal (67) (Figure 1C, Figure S3). We determined HIV-1 expression levels using cell-associated HIV-1 RNA expression from aliquots of 1 million $CD4^+$ T cells. We found that filgotinib, ruxolitinib, spironolactone and mycophenolic acid significantly suppresses cell-associated HIV-1 RNA expression despite PMA/ionomycin challenge with by 1.0 logs, 0.6 logs, 1.5 logs and 0.4 logs, respectively ($p < 0.05$) ex vivo (Figure 1C). Overall, we found that filgotinib and spironolactone inhibits HIV-1 expression more prominently, both in cell line models and in $CD4^+$ T cells from virally suppressed HIV-1-infected individuals.

Filgotinib preferentially suppresses spliced over unspliced HIV-1 transcription

To understand how HIV-1-suppressing agents reduce HIV-1 transcription, we examined whether it is the unspliced HIV-1 RNA, spliced HIV-1 RNA or both that are affected. Using three HIV-1-infected cell line clones (Figure 3A-B) and $CD4^+$ T cells from virally suppressed, HIV-1 infected individuals (Figure 3C-D), we examined the expression levels of cell-associated total HIV-1 RNA (measuring polyadenylated HIV-1 RNA)(68), unspliced HIV-1 RNA (measuring *gag* RNA)(69), and spliced HIV-1 RNA (measuring *tat*/*rev* RNA)(70). We found that these HIV-1-suppressing agents change spliced and unspliced HIV-1 RNA expression differently (Figure 3A). Among them, filgotinib suppresses spliced HIV-1 RNA expression more prominently than unspliced HIV-1 RNA expression (0.7–0.9 log versus 0.2–0.3 log reduction in spliced versus unspliced HIV-1 RNA, respectively)(Figure 3B). In contrast, the other JAK inhibitor ruxolitinib suppresses unspliced but not spliced HIV-1 RNA expression (0.1–0.2 log versus 0.3–0.6 log reduction in spliced versus unspliced HIV-1 RNA, respectively), while spironolactone (0.7–0.8

log versus 0.8–0.9 log reduction) and mycophenolic acid (0.3–0.5 log versus 0.5–0.6 log reduction) suppress both spliced and unspliced HIV-1 RNA expression. We further examined the expression levels of total, unspliced and spliced HIV-1 RNA in $CD4^+$ T cells from virally suppressed, HIV-1-infected individuals challenged with PMA/ionomycin (Figure 3C). We found that filgotinib suppresses the expression of spliced HIV-1 RNA preferentially compared to unspliced HIV-1 RNA (4.1 log versus 0.2 log reduction in spliced versus unspliced HIV-1 RNA, respectively) (Figure 3D). Of note, the low level of *tat/rev* expression in $CD4^+$ cells from ART-suppressed HIV-infected individuals (18) may not provide sufficient dynamic range to determine whether HIV-1-supressing agents reduces spliced HIV-1 RNA transcription, and quantification of *tat-rev* spliced HIV-1 RNA does not capture all spliced HIV-1 RNA species. Therefore, we compared the changes of total HIV-1 RNA and unspliced HIV-1 RNA, which can be readily captured and compared. We found that total HIV-1 RNA level significantly decreased in filgotinib-treated samples (average of 7.5 fold, $p = 0.02$), but unspliced HIV-1 RNA did not have significantly decrease (average of 1.5 fold, $p = 0.4$), indicating that the decrease in total HIV-1 RNA is due to decrease in spliced HIV-1 RNA, consistent with our findings in cell line models. This suggests that filgotinib affect HIV-1 RNA splicing through previously unknown mechanisms different from JAK inhibition (see below).

Filgotinib suppresses HIV-1-driven aberrant host gene transcription

The hallmark of HIV-1-driven aberrant host gene transcription at the integration site is HIV-1-to-host RNA splicing and high levels of host gene transcription downstream but not upstream of the HIV-1 integration site (71). In such event, the host gene transcription is controlled by HIV-1 LTR activity, not host immune homeostasis. When HIV-1 proviruses are integrated into proliferation-related genes, HIV-1-driven aberrant host gene transcription leads to excessive and unchecked proliferation gene expression as a mechanism for HIV-1 integration site-dependent proliferation (71). We hypothesize that inhibiting HIV-1 transcription or splicing

by HIV-1-supressing agents can disrupt HIV-1-driven aberrant host gene transcription. To this end, we examined HIV-1-driven aberrant host gene transcription at the integration site upon treatment with HIV-1-suppressing agents. We used a cell line model (HIV-1-infected Jurkat clone 8B10) in which HIV-1-dsGFP reporter is integrated into the intron of a proliferation related proto-oncogene *VAV1* (71). Integration into *VAV1* is associated with clonal expansion of the HIV-1-infected cells in HIV-1-infected individuals (72) and in lentiviral-transduced CAR T cells (73), suggesting that integration into *VAV1* is a clinically relevant mechanism driving integration site-dependent proliferation in vivo. In this cell line clone, HIV-1 drives high levels of aberrant *VAV1* gene expression through HIV-1 LTR-driven expression and HIV-1-to-*VAV1* splicing (74), particularly downstream but not upstream the HIV-1 integration site (red arrowhead, Figure 4A). This reporter system provides a scalable measurement of HIV-1-driven aberrant host gene expression at the integration site. In mock (DMSO)-treated HIV-1-infected Jurkat clone 8B10, *VAV1* RNA peaks downstream of the HIV-1 integration site are >6 times higher than the RNA peaks upstream the HIV-1 integration site. Treatment with HIV-1-suppressing agents, particularly filgotinib, spironolactone and mycophenolic acid, reduces HIV-1-driven aberrant *VAV1* transcription (Figure 4A). To quantify the effect of HIV-1-suppressing agents on HIV-1-driven aberrant host gene expression, we measured cellular canonical splicing (as measured by RNA reads capturing splicing between *VAV1* exon 1 and exon 2), HIV-1-driven aberrant splicing (as measured by HIV-1-to-host chimeric RNA reads) and HIV-1 RNA expression (as measured by all HIV-1 RNA reads) in the HIV-1-infected Jurkat clone 8B10 (Figure S4). We found that filgotinib, but not other HIV-1-supressing agents, significantly suppresses HIV-driven aberrant splicing to the host RNA by 1 log (Figure S4). Our results demonstrate that the reduction of HIV-1-driven aberrant host gene transcription by filgotinib is mediated through modulating aberrant splicing.

At the protein expression level, HIV-1-driven aberrant *VAV1* transcription leads to a truncated VAV1 protein expression (Figure 4B, ΔVAV1). This is because HIV-1 integrates

downstream the *VAV1* translation start site and obliterates the N-terminal VAV1 protein coding regions. This N-terminal VAV1 truncation removes the regulatory region and increases the oncogenicity of this oncogene (75). Western blot analysis showed that filgotinib, spironolactone, and mycophenolic acid treatment suppresses the oncogenic truncated VAV1 expression (Figure 4B–C). Overall, we showed that HIV-1-suppressing agents not only suppress HIV-1 transcription itself but also disrupt HIV-1-driven aberrant host gene expression at the integration site. To our knowledge, this is the first study showing that HIV-1-driven aberrant host gene expression, a mechanism mediating HIV-1-integration site-dependent proliferation, can be disrupted by FDA-approved drugs.

Transcriptional landscape analysis identifies distinct function of filgotinib on RNA processing

To understand the mechanisms of how HIV-1-suppressing agents suppress HIV-1 RNA expression, we performed transcriptome analysis using three independent methods: 1) Ingenuity pathway analysis (IPA) focusing on differential expression of genes reaching significant statistical difference (76), 2) gene set enrichment analysis (GSEA) focusing on whether *a priori* defined set of genes concordantly differ between two biological states using genome-wide profiling (77), and 3) exon-intron landscape mapping which captures genes affected by changes RNA splicing (78). Different from overexpression or downregulation of individual cellular factors, GSEA allow genome-wide understanding of how drug treatment affects the cellular environment. We compared the transcriptome of HIV-1-infected clone 8B10 Jurkat cell clone (Figure S5A) and $CD4^+$ T cells from virally suppressed HIV-1-infected individuals (Figure 5A) treated with HIV-1-suppressing agents for 24 hours with that of mock (DMSO)-treated cells.

IPA provides standard examination of cellular genes up- or down-regulated during pharmacological perturbations. Using IPA, we found that differentially expressed genes in filgotinib-treated cells, in particular, are strikingly enriched in RNA splicing and RNA processing

(Figure S5B and Figure 5B), which is not seen in cells treated with other HIV-1-suppressing agents (Figure S6).

GSEA, unlike IPA, does not involve filtering out up- or downregulated individual genes based on an arbitrary false discovery rate or p-value. Instead, GSEA examines the transcriptional levels of all the genes involved in candidate cellular pathways (gene sets) and determines whether certain cellular pathways are more prominently affected upon pharmacological perturbations. Using GSEA, we examined all gene ontology (GO) gene sets on molecular signature database (MSigDB)(79) and visualized the pathway interaction networks using EnrichmentMap in Cytoscape (80). Using the highest overlap coefficient, we identified most enriched pathways which may have pivotal influence in the cellular environment (Figure S5C and Figure 5C). Closely clustered GO gene sets represent completely overlapping genes among them, which highlights pathways occurring simultaneously.

We found that the transcriptome signature in filgotinib-treated cells is strikingly different from cells treated with the other JAK inhibitor ruxolitinib and other HIV-1-suppressing agents. First, as a JAK inhibitor, filgotinib suppresses T cell activation, demonstrating downregulation of the JAK-STAT signaling pathway (*STAT6)*, PI3K-Akt pathways (*AKT1*), TCR signaling (*ZAP70* and *IL2RA* (CD25)) and the exhaustion marker *PDCD1* (PD1)(Figure S5D and Figure 5D). While both filgotinib and ruxolitinib are JAK inhibitors, filgotinib-mediated reduction in T cell activation is significantly more prominent.

Second, consistent with IPA analysis (Figure 5B), we found that filgotinib-treated cells upregulate RNA processing-related genes, including RNA splicing (Figure 5E and Figure S5E). Importantly, many of these RNA processing genes have been reported to be critical for HIV-1 transcription, such as *CLK1* (81, 82), *UPF1* (83, 84), *THOC1* (85), *IWS1* (86), and *METTL3* (87). Disrupted RNA expression of these HIV-1-related RNA processing genes may mediate preferential inhibition of HIV-1 splicing (Figure 3).

Third, we found that filgotinib-treated cells have altered chromosome organization and modification pathways (Figure S5F, Figure 5F) which have been reported to affect HIV-1 transcription, such as *TET2* (88), *HDAC1-3* (89-91), *CDK2* (92, 93), *SMYD2* (94), and *BRCA1* (95). Of note, the class I histone deacetylases HDAC1–3, but not other HDACs, induces HIV-1 repression (96). Overall, filgotinib functions not only as a JAK inhibitor that suppresses T cell activation but also inhibits cellular factors involved in HIV-1 transcription, splicing and reactivation. Our finding demonstrates that genome-wide transcriptome analysis systemically can identify potential mechanisms mediating HIV-1 transcription and reactivation.

Filgotinib may potentially function as a splicing inhibitor that induces intron retention

Our finding that filgotinib suppresses spliced HIV-1 RNA expression more prominently than unspliced HIV-1 RNA expression (Figure 3) suggests that filgotinib functions as a splicing inhibitor. During normal cellular splicing events, introns in pre-mRNAs are spliced out, leaving mature mRNA that does not contain introns. When RNA splicing is disrupted, one of the key features is that introns remain in the mature mRNA, a phenomenon called intron retention. Intron retention has emerged as a mechanism of gene expression control (97, 98), in cellular function (99), cancer (100) and HIV-1 infection (101). We examined the impact of filgotinib on RNA splicing using intron retention as a surrogate from the same RNA-seq dataset. Using IRFinder (78), which systemically identifies and quantifies retained introns using bioinformatic calculations, we identified genes harboring retained introns and visualized the exon-intron landscape. Among the four HIV-1-suppressing agents, we found that only filgotinib induces higher frequency of intron retention in both HIV-1-infected Jurkat clone 8B10 and $CD4^+$ T cells from virally suppressed, HIV-1 infected individuals (Figure S7A and Figure 6A). We found that genes harboring retained introns upon filgotinib treatment are enriched in RNA processing and splicing pathways (Figure S7B–H and Figure 6B). In particular, filgotinib induces intron retention in key RNA processing-related genes in HIV-1 transcription, such as *HNRNPH1* (102) and

DDX41 (103) (Figure 6C–F, blue arrowheads). Intron retention in *HNRNPH1* and *DDX41* leads to reduced protein expression (Figure 6G). Our result suggests that filgotinib may potentially functions as a splicing inhibitor to induce intron retention in genes involving HIV-1 RNA processing.

Filgotinib reduces T cell activation upon stimulation

Filgotinib is an immune modulatory agent clinically used to suppresses aberrant T cell activation in autoimmune diseases (Figure 5D). We asked whether JAK inhibition suppresses T cell activation in HIV-1-infeted individuals. We activated $CD4^+$ T cells from virally suppressed, HIV-1-infected individuals with CD3/CD28 stimulation for four days to induced T cell activation and cellular proliferation. The culture was supplemented with ART (tenofovir and enfuvirtide) to prevent new rounds of infection. Cells were treated with DMSO, filgotinib, ruxolitinib, spironolactone or mycophenolic acids for four days, respectively. We found that the JAK inhibitors filgotinib and ruxolitinib and immune modulator mycophenolic acid suppress T cell activation (as measured by CD25 expression) and PD1 expression (Figure S8), while spironolactone does not. Overall, we found that filgotinib suppresses T cell activation both at the transcription level (Figure 5D) and as measured by surface protein expression of activation markers (Figure S8).

Filgotinib reduces the proliferation of HIV-1-infected cells upon T cell activation

To test whether HIV-1-suppressing inhibits the proliferation of HIV-1-infected cells, we tracked cellular proliferation upon CD3/CD28 stimulation using Cell Trace staining (Figure S8). While mycophenolic acids halts proliferation of all $CD4^+$ T cells (<1% proliferated), the JAK inhibitor filgotinib has modest effect on inhibiting proliferation of $CD4^+$ T cells (~49% proliferation).

To test whether HIV-1-suprpessing agents preferentially suppress proliferation of HIV-1-infected cells over uninfected cells, we measured the frequency of cells harboring inducible HIV-1 by the end of CD3/CD28 stimulation. After four days of CD3/CD28 stimulation, we cultured the cells in limiting dilution for 2 days to allow the effect of HIV-1-suppressing agents to be washed out. To determine whether a two-days wash-out period is sufficient to remove HIV-1-suppressing effect, we examined HIV-1-driven GFP expression in the HIV-1-infected Jurkat clone 8B10 after removal of HIV-1-suppressing agents. We found that HIV-1-driven GFP expression returned to basal level within 2 days after drug removal (Figure S9). By measuring the frequency of HIV-1-infected cells over total cells using limiting dilution culture after drug treatment, we will be able to examine whether HIV-1-suppressing agents preferentially reduce proliferation of HIV-1-infected cells over total cells. We then stimulated the cells with PMA/ionomycin to induce maximum latency reversal and measured the frequency of cells harboring inducible HIV-1 using supernatant HIV-1 RNA detection (104, 105). While supernatant HIV-1 RNA expression does not equal the presence of replication competent HIV-1 (28), this cell-free RNA-based inducible RNA assay provides a wide dynamic range to measure the frequency of cells harboring inducible HIV-1 with readouts correlating with quantitative viral outgrowth cultures (104)(Figure 7). We found that filgotinib and mycophenolic acid significantly reduces the frequency of cells harboring inducible HIV-1 (by 0.6 logs and 0.7 logs, respectively). Overall, we found that filgotinib reduces T cell activation and the proliferation of HIV-1-infected cells.

Discussion

The combination of drug screen and three levels of transcriptome analysis (from differential expression, gene set enrichment to exon-intron landscape analysis) systemically identified novel cellular pathways required for HIV-1 transcription as druggable therapeutic targets (Figure 2). Our drug screen not only confirmed previously reported HIV-1 transcription inhibitors but also identified a novel HIV-1-suppressing agent filgotinib. Our transcriptome analysis broadened our understanding on drug effects by genome-wide identification of all pathways involved (Figure 5). Using these transcriptome analyses, we found that filgotinib is not merely a JAK inhibitor. We found a function of filgotinib as a splicing inhibitor, modulating HIV-1 RNA splicing and transcription related cellular factors and mediates preferential suppression of HIV-1 RNA splicing.

We systemically examined the landscape of cellular pathways involved in HIV-1 transcription and respective FDA-approved drugs which target these pathways (Figure 2). We found that both T cell activation pathways and HIV-1 transcription are necessary for full HIV-1 reactivation. We identified additional pathways which can suppress HIV-1 transcription through inhibiting T cell activation-related pathways by using JAK-STAT inhibitors (filgotinib and ruxolitinib), tyrosine kinase inhibitors (dovitinib, pazopanib and ponatinib), Akt inhibitors (uprosertib) and cation transporter inhibitors (digoxin (106), levosimendan (45) and zinc pyrithione). More importantly, we identified RNA transcription pathways involved in HIV-1 transcription, from transcription initiation, elongation, splicing and nuclear export. Transcription initiation requires DNA unwinding by DNA helicase TFIIH (107) and topoisomerases (108) to relieve the supercoiling tension during transcription, which can be inhibited by DNA unwinding inhibitors irinotecan, mitoxantrone and mitomycin C or by the DNA helicase inhibitor spironolactone (50). RNA synthesis requires IMPDH for *de novo* guanosine triphosphate synthesis, which can be inhibited by mycophenolic acid (51). Transcription elongation requires cyclin-dependent kinases (CDK), which can be inhibited by CDK inhibitor flavopiridol. RNA

splicing can be inhibited by filgotinib as a novel splice inhibitor. Finally, nuclear export of unspliced HIV-1 RNA can be inhibited by CRM1 inhibitor KPT-330 (32). We found that filgotinib, as a JAK inhibitor, suppresses T cell activation such as *IL2RA*, *AKT1*, *STAT1*, *VAV1*, and *PDCD1* (Figure 5) as expected. We found filgotinib affects HIV-1 and cellular RNA processing, which can be a new function or an off-target effect. We postulate that this is potentially because that filgotinib, which binds to the ATP binding site at JAK, also binds to RNA processing enzymes. This suggests that combinatorial strategies targeting HIV-1 reactivation pathways can be achieved by one single drug. HIV-1-suppressing agents identified in this study, as a proof of concept, serve as lead compounds for further development of HIV-1-specific therapeutic strategies, likely in combinatorial approaches.

Despite the essential role of RNA splicing (32, 109, 110) in HIV-1 life cycle and pathogenesis, little is known about how targeting HIV-1 RNA splicing can be applied as a therapeutic strategy in the context of HIV-1 persistence (111). Studies have shown that HIV-1 splicing and HIV-1-induced aberrant splicing is associated with HIV-1 persistence (71, 112, 113), which makes RNA splicing an important potential therapeutic target. Different from traditional differential gene expression analysis which identifies a list of up- and down-regulated genes, we broadened transcriptome analysis into qualitative visualization of the RNA transcription landscape. Using RNA landscape approaches, we found that HIV-1-driven cancer-related gene expression can be suppressed by HIV-1-suppressing agents (Figure 4), and we found novel functions of filgotinib as a splicing inhibitor (Figure 6). These new findings in HIV-1-host interactions and HIV-1-drug interactions cannot be found by traditional transcriptome analyses. Our findings highlight the importance of HIV-1 and cellular RNA landscape analysis in studying HIV-1-host interactions and identifying previously unknown mechanisms of drug effects.

Overall, a combination of drug screening and transcriptome analysis identified the landscape of cellular pathways critical for HIV-1 reactivation and a novel HIV-1-suppressing

agent filgotinib. Filgotinib suppresses HIV-1 transcription and reducing the proliferation of HIV-1-infected cells by targeting two different pathways, involving inhibition of T cell activation and modulation of HIV-1-splicing. Therapeutic strategies targeting a combination of these pathways with increased selectivity against HIV-1-infected cells provides a new direction to reduce HIV-1-related immune activation and the expansion of the HIV-1-infected cells.

Materials and Methods

Clinical sample processing

Resting $CD4^+$ T cells from ART-treated, virally suppressed, HIV-1-infected individuals were isolated using magnetic negative depletion (EasySep human $CD4^+$ T cell enrichment kit (STEMCELL, # 17952), CD69 MicroBead Kit, CD25 MicroBead Kit, and HLA-DR Microbead Kit (Miltenyi Biotec)).

Construction of Jurkat T cell clones containing known HIV-1 reporter provirus integration site

Jurkat T cells (NIH AIDS Reagents Program) were transduced with a single-round HIV-1 reporter virus NL4-3-d6-dsEGFP (42) at a low multiplicity of infection (<1% GFP expression). Briefly, full-length NL4-3 genome with part of Env replaced by a destabilized EGFP. Inactivating point mutation were introduced into viral genes except for *tat* and *rev*. This reporter retains TAR, RRE and all splice elements of the NL4-3 backbone. GFP positive cells were sorted three days after infection into single cells and grown into clones. Cell line clones which grew into visible pellets were collected for expansion after three weeks. Integration site of these HIV-1-dsGFP-Jurkat T cell clones were examined using inverse PCR (58, 114). These clones express various levels of HIV-1-driven GFP due to stochastic activation via Tat feedback loop (16) and can be induced to nearly 100% of GFP expression upon PMA (50 ng/ml)/ionomycin (1 μM) stimulation. For dual reporter Jurkat clones, HIV-1-dsGFP-Jurkat clones were transduced with EF1α-driven destabilized BFP containing a nuclear localization signal (NLS) and sorted by BFP positivity three days after transduction.

HIV-1-suppressing agents screen

A small molecule compound library of 1,430 FDA-approved small molecule compounds (Selleckchem, #L1300) were aliquoted to 17 96-well plates for a final concentration of 10 μM for each compound. In each 96-well plate, four wells of flavopiridol served as positive controls and

four wells of DMSO served as negative controls. Cells were fixed and examined under flow cytometry for GFP expression 24 hours after drug treatment.

Drug treatment condition and assays

Dose response curves of HIV-1-dsGFP-Jurkat clones in vitro

All drug treatment was performed at 10 μM unless otherwise specified. Quadruples of 100,000 uninfected Jurkat cells or HIV-1-infected Jurkat T cell clones were seeded in 96-well plates with DMSO, 0.01 μM, 0.1 μM, 1 μM, 2.5 μM, 5 μM, and 10 μM HIV-1-suppressing agents for 24 hours. Cells were stained with LIVE/DEAD Fixable Near-IR Dead Cell Stain Kit (Thermo Fisher, #L10119) and fixed for flow cytometry analysis.

Immune phenotype of $CD4^+$ T cells treated with HIV-1-suppressing agents

$CD4^+$ T cells from virally suppressed, HIV-1-infected individuals were stained with CellTrace Violet (ThermoFisher, #C34571) and activated with Dynabeads human T-activator CD3/CD28 (ThermoFisher), IL-2 (30 U/ml), tenofovir (1 μM) and enfuvirtide (10 μM), and respective HIV-1-suppressing agents (filgotinib, ruxolitinib, spironolactone and mycophenolic acid)(10 μM) or DMSO for 4 days. Cells were stained with anti-CD25-BV605 (clone 2A3, Bio-Rad, #562660), anti-PD1-APC (clone J105, ThermoFisher, #17-2799-42) and LIVE/DEAD Fixable Near-IR Dead Cell Stain Kit (Thermo Fisher, #L10119) for flow cytometric analysis.

RT-qPCR of resting $CD4^+$ T cell from HIV-1-infected individual treated with drugs ex vivo and HIV-1-dsGFP-Jurkat clones

Cells treated with HIV-1-suppressing agents for 24 hours were lysed in TRIzol (1 million cells in 300μl) and total RNA was extracted with Direct-zol RNA miniprep kits (Zymo Research, #R2051). Total (68), unspliced (69) and spliced (115) HIV-1 RNA or cellular RNA (*POLR2A*) was measured by qRT-PCR using qScript XLT 1-Step RT-qPCR ToughMix Low-ROX (Quanta

Bio, #95134-02K) or Taqman Gene Expression Assays (Hs00172187_m1), respectively. Primer probe for total, unspliced, and spliced HIV-1 RNA are: Total RNA (primers: 5'-CAGATGCTGCATATAAGCAGCTG-3' and 5'-TTTTTTTTTTTTTTTTTTTTTTGAAGCACTC-3', probe: 5'FAM-CCTGTACTGGGTCTCTCTGG-Q 3')(68); *gag* (primers: 5'-CATGTTTTCAGCATTATCAGAAGGA-3' and 5'-TGCTTGATGTCCCCCCACT-3', probe: 5'FAM-CCACCCCACAAGATTTAAACACCATGCTAA-Q 3'); *tat/rev* (primers: 5'-CTTAGGCATCTCCTATGGCAGGA-3' and 5'-GGATCTGTCTCTGTCTCTCTCTCCACC-3', probe: 5'FAM-AGGGGACCCGACAGGCCC-Q 3')

Quantification of induced HIV-1 RNA

$CD4^+$ T cells from virally suppressed, HIV-1-infected individuals were treated with Dynabeads human T-activator CD3/CD28 (ThermoFisher, # 111.32D), IL-2 (30 U/ml), tenofovir (1 μM) and enfuvirtide (10 μM), and respective HIV-1-suppressing agents (filgotinib, ruxolitinib, spironolactone and mycophenolic acid)(10 μM) or DMSO for 4 days. Cells were then pelleted to remove HIV-1-suppressing agents and plated at limiting dilution (200,000 cells per well). After two days of wash-out period allowing the effect of HIV-1-suppressing agents to decline, culture supernatant of each of the limiting dilution wells was collected for RNA extraction and supernatant RT-qPCR of HIV-1 *gag*, as modified from an inducible HIV-1 RNA assay (104).

<u>RNA-seq analysis</u>

RNA extraction and library construction

Samples treated with HIV-1-suppresing agents for 24 hours were collected for total RNA isolation using TRIzol (ThermoFisher) following Direct-zol RNA extraction kit (Zymo). Approximately 500 ng of total RNA was used to generate cDNA library using TruSeq mRNA Library Prep kit (Illumina) for Illumina HiSeq 4000 2x100 bp sequencing or NEBNext Ultra II directional mRNA library prep kit (NEB) for Novaseq 6000 2x150 bp sequencing.

Trimming and alignment

Low quality reads from raw fastq files were trimmed using Trimomatic with “LEADING:3 TRAILING:3 SLIDINGWINDOW:4:30 MINLEN:50” arguments. Trimmed fastq files were aligned using STAR 2.6.1d or 2.7.0f with the following arguments: “ --readFilesCommand gunzip -c --outSAMtype BAM SortedByCoordinate --chimOutType SeparateSAMold --runThreadN 20 --outFilterType BySJout --alignSJoverhangMin 5 --alignSJDBoverhangMin 3 --chimSegmentMin 15 --outSAMstrandField intronMotif --outSAMattributes All --quantMode GeneCounts” to customized human assembly hg38 release 91 plus HIV-1 sequence (HXB2 or HIV-1-dsGFP).

Pathway enrichment on differential expressed genes

Total gene count and normalization of STAR aligned bam file was obtained using HTseq (htseq-count -r pos -f bam -s reverse) and DESeq2 with human genome assembly hg38 release 91. Genes with the sum of read count smaller than 10 were filtered out. Differentially expressed genes were analyzed with adjusted *p*-value < 0.05 and fold change over $\log_2$ of 1.6 (3 fold). Disease and biological function pathway analysis was carried out using ingenuity pathway analysis (IPA) with the following analysis setting: Species, Human; Tissues and Cell, Immune cells, other cells, other tissues and primary cells, immune cell lines, other cell line. Top ten enriched pathways were presented in this article.

Gene Set Enrichment Analysis and visualization

Total gene count and normalization of STAR aligned bam file was obtained using HTseq (htseq-count -r pos -f bam -s reverse) and DESeq2 with human genome assembly hg38 release 91. Gene with the sum of read count smaller than 10 was filtered out. Normalized counts were analyzed using GSEA (4.0.2) desktop software with c5.all.v7.symbols.gmt [Gene ontology] gene sets database, 1000 number of permutations, No_Collapse, phenotype of permutation type, and

Human_ENSEMBL_Gene_ID_MSigDBv7.0.chip. The result was then visualized using EnrichmentMap in Cytoscape with FDR < 0.25, *p*-value < 0.005, overlap efficiency equals 1. Top clustered were selected by selecting nodes which have the largest number of immediate neighbors.

Intron retention (IR) analysis

Quality trimmed fastq files were analyzed with IRFinder 1.2.5 using STAR-built indexes with human genome assembly hg38 release 91.gtf as reference annotation (78). Up to triplicates of treatments were compared. Output files were filtered with following criteria in Rstudio (1.1.463): `A-IRratio` >= 0.1 & `A-IntronCover` >= 0.7 & `A-IntronDepth` >= 6 & `A-SplicesExact` >= 2 & `B-IRratio` < 0.1 & `B-SplicesExact` >=2. Unequal variance *t*-test of IRratio between two treatment groups were applied and intron-retained regions with significant difference ($p < 0.05$) were reported.

Western blot

Anti-VAV1 antibody (clone 2E11, ThermoFisher, #MA5-17198), anti-GAPDH antibody (clone GA1R, ThermoFisher, # MA5-15738), anti-HNRNPH1 antibody (clone OTI4F10, ThermoFisher, #MA5-27375 and anti-DDX41 antibody (clone C-3, Santa Cruze, #sc-166225) were used in this study.

Statistical analysis

We first performed normality test using Shapiro-Wilk and Kolmogorov-Smirnov test in Prism. Samples treated in independent culture wells were each compared with controls and were not corrected by multiple comparisons. For HIV-1 RNA copy numbers from cells from HIV-infected individuals which were discontinuous and did not follow Gaussian distribution, Wilcoxon rank-sum tests were used to compare two groups (PMA/ionomycin to DMSO control) between paired

clinical samples results which do not follow Gaussian distribution. In multiple groups of discontinuous variables which have arbitrary detection limits, such as RT-qPCR results and the frequency of HIV-1-infected cells, nonparametric ANOVA Friedman's test (two-tailed) with uncorrected Dunn's test was used to compare multi-group (treatment compared to DMSO control). Western blot quantification followed Gaussian distribution and was tested by one-way ANOVA with Fisher's LSD test. For the measurement of cellular canonical splicing, HIV-1-driven aberrant splicing and HIV-1 RNA transcription, RNA reads came from the same RNA-seq sample and were normalized by multiple comparison tests: repeated measure two-way ANOVA with the Geisser-Greenhouse correction and a post hoc analysis with Dunnett's multiple comparisons test were used. All statistical calculations were done with Prism v8.4 (GraphPad). *p*-values <0.05 were considered significant.

Study approval

The Yale University Institutional Review Board approved this study. All participants were provided with written consent. All HIV-1-infected individuals enrolled were on suppressive ART and maintained undetectable plasma HIV-1 RNA levels (<50 copies/ml) for at least 6 months prior to enrollment. Characteristics of HIV-1-infected individuals are listed in Table S2.

Author contributions

Conceptualization and experimental design: Y.-C.H, Y.-H.Y. Experimental investigation: HIV-1-infected Jurkat T cell clones: Y.-C.H. Drug screen: Y.-C.H., K.J. Dose response curve: K.J, Y.-H.Y. In vitro and ex vivo study: Y.-H.Y. Bioinformatic analysis: Y.-H.Y. Study participant recruitment: R.C., J.C., R.H., S.G.D. Writing: Y.-C.H, Y.-H.Y., S.G.D.

Acknowledgments

We thank all study participants. We thank NIH AIDS Reagents Program. **Funding**: This work is supported by Yale Top Scholar, Rudolf J. Anderson Fellowship, NIH R01 AI141009 (Y.-C.H.), R61 DA047037 (Y.-C.H.), R21AI118402 (Y.-C.H.), R37AI147868 (Y.-C.H), W. W. Smith AIDS Research Grant (Y.-C.H.), Johns Hopkins Center for AIDS Research Award P30AI094189 (Y.-C.H.), Gilead AIDS Research Grant (Y.-C.H.), Gilead HIV Research Scholar Grant (Y.-C.H.), NIH BEAT-HIV Delaney Collaboratory UM1AI126620 (Y.-C.H.) and NIH CHEETAH P50 AI150464-13 (Y.-C.H.). The SCOPE cohort was supported by the UCSF/Gladstone Institute of Virology & Immunology CFAR (P30 AI027763) and the CFAR Network of Integrated Systems (R24 AI067039). Additional support was provided by the Delaney AIDS Research Enterprise (DARE; AI096109, A127966). **Data and materials availability**: RNA-seq results are available at GEO (GSE149353).

References and Notes:

1. Finzi D, Hermankova M, Pierson T, Carruth LM, Buck C, Chaisson RE, et al. Identification of a reservoir for HIV-1 in patients on highly active antiretroviral therapy. *Science.* 1997;278(5341):1295-300.
2. Wong JK, Hezareh M, Gunthard HF, Havlir DV, Ignacio CC, Spina CA, et al. Recovery of replication-competent HIV despite prolonged suppression of plasma viremia. *Science.* 1997;278(5341):1291-5.
3. Chun TW, Stuyver L, Mizell SB, Ehler LA, Mican JA, Baseler M, et al. Presence of an inducible HIV-1 latent reservoir during highly active antiretroviral therapy. *Proc Natl Acad Sci U S A.* 1997;94(24):13193-7.
4. De Scheerder MA, Vrancken B, Dellicour S, Schlub T, Lee E, Shao W, et al. HIV Rebound Is Predominantly Fueled by Genetically Identical Viral Expansions from Diverse Reservoirs. *Cell Host Microbe.* 2019;26(3):347-58 e7.
5. Archin NM, Liberty AL, Kashuba AD, Choudhary SK, Kuruc JD, Crooks AM, et al. Administration of vorinostat disrupts HIV-1 latency in patients on antiretroviral therapy. *Nature.* 2012;487(7408):482-5.
6. Korin YD, Brooks DG, Brown S, Korotzer A, and Zack JA. Effects of prostratin on T-cell activation and human immunodeficiency virus latency. *J Virol.* 2002;76(16):8118-23.
7. Nixon CC, Mavigner M, Sampey GC, Brooks AD, Spagnuolo RA, Irlbeck DM, et al. Systemic HIV and SIV latency reversal via non-canonical NF-kappaB signalling in vivo. *Nature.* 2020;578(7793):160-5.
8. McBrien JB, Mavigner M, Franchitti L, Smith SA, White E, Tharp GK, et al. Robust and persistent reactivation of SIV and HIV by N-803 and depletion of CD8(+) cells. *Nature.* 2020;578(7793):154-9.

9. Rasmussen TA, Tolstrup M, Brinkmann CR, Olesen R, Erikstrup C, Solomon A, et al. Panobinostat, a histone deacetylase inhibitor, for latent-virus reactivation in HIV-infected patients on suppressive antiretroviral therapy: a phase 1/2, single group, clinical trial. *Lancet HIV.* 2014;1(1):e13-21.
10. Wei DG, Chiang V, Fyne E, Balakrishnan M, Barnes T, Graupe M, et al. Histone Deacetylase Inhibitor Romidepsin Induces HIV Expression in CD4 T Cells from Patients on Suppressive Antiretroviral Therapy at Concentrations Achieved by Clinical Dosing. *Plos Pathogens.* 2014;10(4):e1004071.
11. Mota TM, McCann CD, Danesh A, Huang S-H, Magat DB, Ren Y, et al. Integrated assessment of viral transcription, antigen presentation, and CD8+ T cell function reveal multiple limitations of class I selective HDACi during HIV-1 latency reversal. *Journal of Virology.* 2020:JVI.01845-19.
12. Boucau J, Madouasse J, Kourjian G, Carlin CS, Wambua D, Berberich MJ, et al. The Activation State of CD4 T Cells Alters Cellular Peptidase Activities, HIV Antigen Processing, and MHC Class I Presentation in a Sequence-Dependent Manner. *The Journal of Immunology.* 2019:ji1700950.
13. Bohnlein E, Lowenthal JW, Siekevitz M, Ballard DW, Franza BR, and Greene WC. The Same Inducible Nuclear Proteins Regulates Mitogen Activation of Both the Interleukin-2 Receptor-Alpha Gene and Type-1 Hiv. *Cell.* 1988;53(5):827-36.
14. Jones KA, and Peterlin BM. Control of Rna Initiation and Elongation at the Hiv-1 Promoter. *Annual Review of Biochemistry.* 1994;63:717-43.
15. Tyagi M, Pearson RJ, and Karn J. Establishment of HIV Latency in Primary CD4(+) Cells Is due to Epigenetic Transcriptional Silencing and P-TEFb Restriction. *Journal of Virology.* 2010;84(13):6425-37.
16. Weinberger LS, Burnett JC, Toettcher JE, Arkin AP, and Schaffer DV. Stochastic gene expression in a lentiviral positive-feedback loop: HIV-1 Tat fluctuations drive phenotypic diversity. *Cell.* 2005;122(2):169-82.
17. West MJ, Lowe AD, and Karn J. Activation of human immunodeficiency virus transcription in T cells revisited: NF-kappaB p65 stimulates transcriptional elongation. *J Virol.* 2001;75(18):8524-37.
18. Yukl SA, Kaiser P, Kim P, Telwatte S, Joshi SK, Vu M, et al. HIV latency in isolated patient CD4(+) T cells may be due to blocks in HIV transcriptional elongation, completion, and splicing. *Sci Transl Med.* 2018;10(430).
19. Coull JJ, Romerio F, Sun JM, Volker JL, Galvin KM, Davie JR, et al. The human factors YY1 and LSF repress the human immunodeficiency virus type 1 long terminal repeat via recruitment of histone deacetylase 1. *J Virol.* 2000;74(15):6790-9.
20. Kauder SE, Bosque A, Lindqvist A, Planelles V, and Verdin E. Epigenetic regulation of HIV-1 latency by cytosine methylation. *PLoS Pathog.* 2009;5(6):e1000495.
21. Van Lint C, Emiliani S, Ott M, and Verdin E. Transcriptional activation and chromatin remodeling of the HIV-1 promoter in response to histone acetylation. *EMBO J.* 1996;15(5):1112-20.
22. Einkauf KB, Lee GQ, Gao C, Sharaf R, Sun X, Hua S, et al. Intact HIV-1 proviruses accumulate at distinct chromosomal positions during prolonged antiretroviral therapy. *J Clin Invest.* 2019;129(3):988-98.
23. Roebuck KA, Gu DS, and Kagnoff MF. Activating protein-1 cooperates with phorbol ester activation signals to increase HIV-1 expression. *Aids.* 1996;10(8):819-26.
24. Kinoshita S, Su L, Amano M, Timmerman LA, Kaneshima H, and Nolan GP. The T cell activation factor NF-ATc positively regulates HIV-1 replication and gene expression in T cells. *Immunity.* 1997;6(3):235-44.
25. Nabel G, and Baltimore D. An inducible transcription factor activates expression of human immunodeficiency virus in T cells. *Nature.* 1987;326(6114):711-3.

26. Fennessey CM, Pinkevych M, Immonen TT, Reynaldi A, Venturi V, Nadella P, et al. Genetically-barcoded SIV facilitates enumeration of rebound variants and estimation of reactivation rates in nonhuman primates following interruption of suppressive antiretroviral therapy. *PLoS Pathog.* 2017;13(5):e1006359.
27. Pinkevych M, Cromer D, Tolstrup M, Grimm AJ, Cooper DA, Lewin SR, et al. HIV Reactivation from Latency after Treatment Interruption Occurs on Average Every 5-8 Days--Implications for HIV Remission. *PLoS Pathog.* 2015;11(7):e1005000.
28. Pollack RA, Jones RB, Pertea M, Bruner KM, Martin AR, Thomas AS, et al. Defective HIV-1 Proviruses Are Expressed and Can Be Recognized by Cytotoxic T Lymphocytes, which Shape the Proviral Landscape. *Cell Host & Microbe.* 2017;21(4):494-+.
29. Kearney MF, Wiegand A, Shao W, Coffin JM, Mellors JW, Lederman M, et al. Origin of Rebound Plasma HIV Includes Cells with Identical Proviruses That Are Transcriptionally Active before Stopping of Antiretroviral Therapy. *J Virol.* 2016;90(3):1369-76.
30. Hunt PW, Martin JN, Sinclair E, Bredt B, Hagos E, Lampiris H, et al. T cell activation is associated with lower CD4(+) T cell gains in human immunodeficiency virus-infected patients with sustained viral suppression during antiretroviral therapy. *Journal of Infectious Diseases.* 2003;187(10):1534-43.
31. Hunt PW, Brenchley J, Sinclair E, McCune JM, Roland M, Page-Shafer K, et al. Relationship between T cell activation and CD4(+) T cell count in HIV-seropositive individuals with undetectable plasma HIV RNA levels in the absence of therapy. *Journal of Infectious Diseases.* 2008;197(1):126-33.
32. Akiyama H, Miller CM, Ettinger CR, Belkina AC, Snyder-Cappione JE, and Gummuluru S. HIV-1 intron-containing RNA expression induces innate immune activation and T cell dysfunction. *Nat Commun.* 2018;9(1):3450.
33. McCauley SM, Kim K, Nowosielska A, Dauphin A, Yurkovetskiy L, Diehl WE, et al. Intron-containing RNA from the HIV-1 provirus activates type I interferon and inflammatory cytokines. *Nat Commun.* 2018;9(1):5305.
34. Hatano H, Jain V, Hunt PW, Lee TH, Sinclair E, Do TD, et al. Cell-based measures of viral persistence are associated with immune activation and programmed cell death protein 1 (PD-1)-expressing CD4+ T cells. *J Infect Dis.* 2013;208(1):50-6.
35. Lederman MM, Funderburg NT, Sekaly RP, Klatt NR, and Hunt PW. Residual immune dysregulation syndrome in treated HIV infection. *Adv Immunol.* 2013;119:51-83.
36. Hunt PW, Lee SA, and Siedner MJ. Immunologic Biomarkers, Morbidity, and Mortality in Treated HIV Infection. *J Infect Dis.* 2016;214 Suppl 2:S44-50.
37. Hsue PY, Lo JC, Franklin A, Bolger AF, Martin JN, Deeks SG, et al. Progression of atherosclerosis as assessed by carotid intima-media thickness in patients with HIV infection. *Circulation.* 2004;109(13):1603-8.
38. Hsue PY, Deeks SG, and Hunt PW. Immunologic basis of cardiovascular disease in HIV-infected adults. *J Infect Dis.* 2012;205 Suppl 3:S375-82.
39. Deeks SG. Immune dysfunction, inflammation, and accelerated aging in patients on antiretroviral therapy. *Top HIV Med.* 2009;17(4):118-23.
40. Hodes RJ, Sierra F, Austad SN, Epel E, Neigh GN, Erlandson KM, et al. Disease drivers of aging. *Ann N Y Acad Sci.* 2016;1386(1):45-68.
41. Wang Y, Lifshitz L, Gellatly K, Vinton CL, Busman-Sahay K, McCauley S, et al. HIV-1-induced cytokines deplete homeostatic innate lymphoid cells and expand TCF7-dependent memory NK cells. *Nature Immunology.* 2020.
42. Yang HC, Xing SF, Shan L, O'Connell K, Dinoso J, Shen AD, et al. Small-molecule screening using a human primary cell model of HIV latency identifies compounds that reverse latency without cellular activation. *Journal of Clinical Investigation.* 2009;119(11):3473-86.

43. Yang HC, Shen L, Siliciano RF, and Pomerantz JL. Isolation of a cellular factor that can reactivate latent HIV-1 without T cell activation. *Proceedings of the National Academy of Sciences of the United States of America.* 2009;106(15):6321-6.
44. Zhu J, Gaiha GD, John SP, Pertel T, Chin CR, Gao G, et al. Reactivation of latent HIV-1 by inhibition of BRD4. *Cell Rep.* 2012;2(4):807-16.
45. Hayashi T, Jean M, Huang H, Simpson S, Santoso NG, and Zhu J. Screening of an FDA-approved compound library identifies levosimendan as a novel anti-HIV-1 agent that inhibits viral transcription. *Antiviral Res.* 2017;146:76-85.
46. Laird GM, Eisele EE, Rabi SA, Nikolaeva D, and Siliciano RF. A novel cell-based high-throughput screen for inhibitors of HIV-1 gene expression and budding identifies the cardiac glycosides. *J Antimicrob Chemother.* 2014;69(4):988-94.
47. Mousseau G, and Valente S. Strategies to Block HIV Transcription: Focus on Small Molecule Tat Inhibitors. *Biology (Basel).* 2012;1(3):668-97.
48. Besnard E, Hakre S, Kampmann M, Lim HW, Hosmane NN, Martin A, et al. The mTOR Complex Controls HIV Latency. *Cell Host Microbe.* 2016;20(6):785-97.
49. Das B, Dobrowolski C, Luttge B, Valadkhan S, Chomont N, Johnston R, et al. Estrogen receptor-1 is a key regulator of HIV-1 latency that imparts gender-specific restrictions on the latent reservoir. *Proc Natl Acad Sci U S A.* 2018;115(33):E7795-E804.
50. Lacombe B, Morel M, Margottin-Goguet F, and Ramirez BC. Specific Inhibition of HIV Infection by the Action of Spironolactone in T Cells. *J Virol.* 2016;90(23):10972-80.
51. Chapuis AG, Paolo Rizzardi G, D'Agostino C, Attinger A, Knabenhans C, Fleury S, et al. Effects of mycophenolic acid on human immunodeficiency virus infection in vitro and in vivo. *Nat Med.* 2000;6(7):762-8.
52. Gavegnano C, Brehm JH, Dupuy FP, Talla A, Ribeiro SP, Kulpa DA, et al. Novel mechanisms to inhibit HIV reservoir seeding using Jak inhibitors. *PLoS Pathog.* 2017;13(12):e1006740.
53. Genovese MC, Kalunian K, Gottenberg JE, Mozaffarian N, Bartok B, Matzkies F, et al. Effect of Filgotinib vs Placebo on Clinical Response in Patients With Moderate to Severe Rheumatoid Arthritis Refractory to Disease-Modifying Antirheumatic Drug Therapy: The FINCH 2 Randomized Clinical Trial. *JAMA.* 2019;322(4):315-25.
54. van der Heijde D, Baraliakos X, Gensler LS, Maksymowych WP, Tseluyko V, Nadashkevich O, et al. Efficacy and safety of filgotinib, a selective Janus kinase 1 inhibitor, in patients with active ankylosing spondylitis (TORTUGA): results from a randomised, placebo-controlled, phase 2 trial. *Lancet.* 2018;392(10162):2378-87.
55. Mease P, Coates LC, Helliwell PS, Stanislavchuk M, Rychlewska-Hanczewska A, Dudek A, et al. Efficacy and safety of filgotinib, a selective Janus kinase 1 inhibitor, in patients with active psoriatic arthritis (EQUATOR): results from a randomised, placebo-controlled, phase 2 trial. *Lancet.* 2018;392(10162):2367-77.
56. Vermeire S, Schreiber S, Petryka R, Kuehbacher T, Hebuterne X, Roblin X, et al. Clinical remission in patients with moderate-to-severe Crohn's disease treated with filgotinib (the FITZROY study): results from a phase 2, double-blind, randomised, placebo-controlled trial. *Lancet.* 2017;389(10066):266-75.
57. Schroder AR, Shinn P, Chen H, Berry C, Ecker JR, and Bushman F. HIV-1 integration in the human genome favors active genes and local hotspots. *Cell.* 2002;110(4):521-9.
58. Han YF, Lassen K, Monie D, Sedaghat AR, Shimoji S, Liu X, et al. Resting CD4(+) T cells from human immunodeficiency virus type I (HIV-1)-infected individuals carry integrated HIV-1 Genomes within actively transcribed host genes. *Journal of Virology.* 2004;78(12):6122-33.
59. Gavegnano C, Detorio M, Montero C, Bosque A, Planelles V, and Schinazi RF. Ruxolitinib and tofacitinib are potent and selective inhibitors of HIV-1 replication and virus reactivation in vitro. *Antimicrob Agents Chemother.* 2014;58(4):1977-86.

60. Chao SH, Fujinaga K, Marion JE, Taube R, Sausville EA, Senderowicz AM, et al. Flavopiridol inhibits P-TEFb and blocks HIV-1 replication. *J Biol Chem.* 2000;275(37):28345-8.
61. Martin AR, Pollack RA, Capoferri A, Ambinder RF, Durand CM, and Siliciano RF. Rapamycin-mediated mTOR inhibition uncouples HIV-1 latency reversal from cytokine-associated toxicity. *J Clin Invest.* 2017;127(2):651-6.
62. Contreras X, Barboric M, Lenasi T, and Peterlin BM. HMBA releases P-TEFb from HEXIM1 and 7SK snRNA via PI3K/Akt and activates HIV transcription. *PLoS Pathog.* 2007;3(10):1459-69.
63. Daelemans D, Afonina E, Nilsson J, Werner G, Kjems J, De Clercq E, et al. A synthetic HIV-1 Rev inhibitor interfering with the CRM1-mediated nuclear export. *Proc Natl Acad Sci U S A.* 2002;99(22):14440-5.
64. Reeves DB, Duke ER, Hughes SM, Prlic M, Hladik F, and Schiffer JT. Anti-proliferative therapy for HIV cure: a compound interest approach. *Sci Rep.* 2017;7(1):4011.
65. Vanhoutte F, Mazur M, Voloshyn O, Stanislavchuk M, Van der Aa A, Namour F, et al. Efficacy, Safety, Pharmacokinetics, and Pharmacodynamics of Filgotinib, a Selective JAK-1 Inhibitor, After Short-Term Treatment of Rheumatoid Arthritis: Results of Two Randomized Phase IIa Trials. *Arthritis Rheumatol.* 2017;69(10):1949-59.
66. Karim A, Zagarella J, Hutsell TC, Chao A, and Baltes BJ. Spironolactone. II. Bioavailability. *Clin Pharmacol Ther.* 1976;19(2):170-6.
67. Bullen CK, Laird GM, Durand CM, Siliciano JD, and Siliciano RF. New ex vivo approaches distinguish effective and ineffective single agents for reversing HIV-1 latency in vivo. *Nat Med.* 2014;20(4):425-9.
68. Shan L, Rabi SA, Laird GM, Eisele EE, Zhang H, Margolick JB, et al. A novel PCR assay for quantification of HIV-1 RNA. *J Virol.* 2013;87(11):6521-5.
69. Palmer S, Wiegand AP, Maldarelli F, Bazmi H, Mican JM, Polis M, et al. New real-time reverse transcriptase-initiated PCR assay with single-copy sensitivity for human immunodeficiency virus type 1 RNA in plasma. *J Clin Microbiol.* 2003;41(10):4531-6.
70. Massanella M, Gianella S, Lada SM, Richman DD, and Strain MC. Quantification of Total and 2-LTR (Long terminal repeat) HIV DNA, HIV RNA and Herpesvirus DNA in PBMCs. *Bio Protoc.* 2015;5(11).
71. Runxia Liu† Y-HJY, Ales Varabyou†, Jack A. Collora, Scott Sherrill-Mix, C. Conover Talbot Jr., Sameet Mehta, Kristen Albrecht, Haiping Hao, Hao Zhang, Ross A. Pollack, Subul A. Beg, Rachela M. Calvi, Jianfei Hu, Christine M. Durand, Richard F. Ambinder, Rebecca Hoh, Steven G. Deeks, Jennifer Chiarella, Serena Spudich, Daniel C. Douek, Frederic D. Bushman, Mihaela Pertea, Ya-Chi Ho. Single-cell transcriptional landscape reveals HIV-1-driven aberrant host gene transcription as a therapeutic target. *Science Translational Medicine.* 2020;in Press.
72. Maldarelli F, Wu X, Su L, Simonetti FR, Shao W, Hill S, et al. HIV latency. Specific HIV integration sites are linked to clonal expansion and persistence of infected cells. *Science.* 2014;345(6193):179-83.
73. Nobles CL, Sherrill-Mix S, Everett JK, Reddy S, Fraietta JA, Porter DL, et al. CD19-targeting CAR T cell immunotherapy outcomes correlate with genomic modification by vector integration. *The Journal of Clinical Investigation.* 2019;130(2).
74. Liu R, Yeh Y-HJ, Varabyou A, Collora JA, Sherrill-Mix S, Talbot CCJ, et al. Single-cell transcriptional landscapes reveal HIV-1-driven aberrant host gene transcription as a potential therapeutic target. *Science Translational Medicine.* 2019;Accepted.
75. Katzav S, Cleveland JL, Heslop HE, and Pulido D. Loss of the amino-terminal helix-loop-helix domain of the vav proto-oncogene activates its transforming potential. *Mol Cell Biol.* 1991;11(4):1912-20.

76. Kramer A, Green J, Pollard J, Jr., and Tugendreich S. Causal analysis approaches in Ingenuity Pathway Analysis. *Bioinformatics.* 2014;30(4):523-30.
77. Subramanian A, Tamayo P, Mootha VK, Mukherjee S, Ebert BL, Gillette MA, et al. Gene set enrichment analysis: a knowledge-based approach for interpreting genome-wide expression profiles. *Proc Natl Acad Sci U S A.* 2005;102(43):15545-50.
78. Middleton R, Gao D, Thomas A, Singh B, Au A, Wong JJ, et al. IRFinder: assessing the impact of intron retention on mammalian gene expression. *Genome Biol.* 2017;18(1):51.
79. Liberzon A, Subramanian A, Pinchback R, Thorvaldsdottir H, Tamayo P, and Mesirov JP. Molecular signatures database (MSigDB) 3.0. *Bioinformatics.* 2011;27(12):1739-40.
80. Shannon P, Markiel A, Ozier O, Baliga NS, Wang JT, Ramage D, et al. Cytoscape: a software environment for integrated models of biomolecular interaction networks. *Genome Res.* 2003;13(11):2498-504.
81. Wong RW, Balachandran A, Ostrowski MA, and Cochrane A. Digoxin suppresses HIV-1 replication by altering viral RNA processing. *PLoS Pathog.* 2013;9(3):e1003241.
82. Wong R, Balachandran A, Mao AY, Dobson W, Gray-Owen S, and Cochrane A. Differential effect of CLK SR Kinases on HIV-1 gene expression: potential novel targets for therapy. *Retrovirology.* 2011;8:47.
83. Serquina AK, Das SR, Popova E, Ojelabi OA, Roy CK, and Gottlinger HG. UPF1 is crucial for the infectivity of human immunodeficiency virus type 1 progeny virions. *J Virol.* 2013;87(16):8853-61.
84. Ajamian L, Abrahamyan L, Milev M, Ivanov PV, Kulozik AE, Gehring NH, et al. Unexpected roles for UPF1 in HIV-1 RNA metabolism and translation. *RNA.* 2008;14(5):914-27.
85. Pak V, Eifler TT, Jager S, Krogan NJ, Fujinaga K, and Peterlin BM. CDK11 in TREX/THOC Regulates HIV mRNA 3' End Processing. *Cell Host Microbe.* 2015;18(5):560-70.
86. Yoh SM, Lucas JS, and Jones KA. The Iws1:Spt6:CTD complex controls cotranscriptional mRNA biosynthesis and HYPB/Setd2-mediated histone H3K36 methylation. *Genes Dev.* 2008;22(24):3422-34.
87. Lichinchi G, Gao S, Saletore Y, Gonzalez GM, Bansal V, Wang Y, et al. Dynamics of the human and viral m(6)A RNA methylomes during HIV-1 infection of T cells. *Nat Microbiol.* 2016;1:16011.
88. Lv L, Wang Q, Xu Y, Tsao LC, Nakagawa T, Guo H, et al. Vpr Targets TET2 for Degradation by CRL4(VprBP) E3 Ligase to Sustain IL-6 Expression and Enhance HIV-1 Replication. *Mol Cell.* 2018;70(5):961-70 e5.
89. Sorin M, Cano J, Das S, Mathew S, Wu X, Davies KP, et al. Recruitment of a SAP18-HDAC1 complex into HIV-1 virions and its requirement for viral replication. *PLoS Pathog.* 2009;5(6):e1000463.
90. Margolis DM. Histone deacetylase inhibitors and HIV latency. *Curr Opin HIV AIDS.* 2011;6(1):25-9.
91. Barton KM, Archin NM, Keedy KS, Espeseth AS, Zhang YL, Gale J, et al. Selective HDAC inhibition for the disruption of latent HIV-1 infection. *PLoS One.* 2014;9(8):e102684.
92. Pauls E, Ruiz A, Badia R, Permanyer M, Gubern A, Riveira-Munoz E, et al. Cell cycle control and HIV-1 susceptibility are linked by CDK6-dependent CDK2 phosphorylation of SAMHD1 in myeloid and lymphoid cells. *J Immunol.* 2014;193(4):1988-97.
93. Ammosova T, Berro R, Jerebtsova M, Jackson A, Charles S, Klase Z, et al. Phosphorylation of HIV-1 Tat by CDK2 in HIV-1 transcription. *Retrovirology.* 2006;3:78.
94. Boehm D, Jeng M, Camus G, Gramatica A, Schwarzer R, Johnson JR, et al. SMYD2-Mediated Histone Methylation Contributes to HIV-1 Latency. *Cell Host Microbe.* 2017;21(5):569-79 e6.

95. Guendel I, Meltzer BW, Baer A, Dever SM, Valerie K, Guo J, et al. BRCA1 functions as a novel transcriptional cofactor in HIV-1 infection. *Virol J.* 2015;12:40.
96. Keedy KS, Archin NM, Gates AT, Espeseth A, Hazuda DJ, and Margolis DM. A limited group of class I histone deacetylases acts to repress human immunodeficiency virus type 1 expression. *J Virol.* 2009;83(10):4749-56.
97. Hao S, and Baltimore D. RNA splicing regulates the temporal order of TNF-induced gene expression. *Proc Natl Acad Sci U S A.* 2013;110(29):11934-9.
98. Ni T, Yang W, Han M, Zhang Y, Shen T, Nie H, et al. Global intron retention mediated gene regulation during CD4+ T cell activation. *Nucleic Acids Res.* 2016;44(14):6817-29.
99. Braunschweig U, Barbosa-Morais NL, Pan Q, Nachman EN, Alipanahi B, Gonatopoulos-Pournatzis T, et al. Widespread intron retention in mammals functionally tunes transcriptomes. *Genome Res.* 2014;24(11):1774-86.
100. Frankiw L, Majumdar D, Burns C, Vlach L, Moradian A, Sweredoski MJ, et al. BUD13 Promotes a Type I Interferon Response by Countering Intron Retention in Irf7. *Mol Cell.* 2019;73(4):803-14 e6.
101. Sherrill-Mix S, Ocwieja KE, and Bushman FD. Gene activity in primary T cells infected with HIV89.6: intron retention and induction of genomic repeats. *Retrovirology.* 2015;12:79.
102. Kutluay SB, Emery A, Penumutchu SR, Townsend D, Tenneti K, Madison MK, et al. Genome-Wide Analysis of Heterogeneous Nuclear Ribonucleoprotein (hnRNP) Binding to HIV-1 RNA Reveals a Key Role for hnRNP H1 in Alternative Viral mRNA Splicing. *Journal of Virology.* 2019;93(21):e01048-19.
103. Stavrou S, Aguilera AN, Blouch K, and Ross SR. DDX41 Recognizes RNA/DNA Retroviral Reverse Transcripts and Is Critical for In Vivo Control of Murine Leukemia Virus Infection. *mBio.* 2018;9(3):e00923-18.
104. Massanella M, Yek C, Lada SM, Nakazawa M, Shefa N, Huang K, et al. Improved assays to measure and characterize the inducible HIV reservoir. *EBioMedicine.* 2018;36:113-21.
105. Rosenbloom DI, Elliott O, Hill AL, Henrich TJ, Siliciano JM, and Siliciano RF. Designing and Interpreting Limiting Dilution Assays: General Principles and Applications to the Latent Reservoir for Human Immunodeficiency Virus-1. *Open Forum Infect Dis.* 2015;2(4):ofv123.
106. Zhyvoloup A, Melamed A, Anderson I, Planas D, Lee CH, Kriston-Vizi J, et al. Digoxin reveals a functional connection between HIV-1 integration preference and T-cell activation. *PLoS Pathog.* 2017;13(7):e1006460.
107. Dvir A, Conaway RC, and Conaway JW. A role for TFIIH in controlling the activity of early RNA polymerase II elongation complexes. *Proc Natl Acad Sci U S A.* 1997;94(17):9006-10.
108. Mondal N, and Parvin JD. DNA topoisomerase IIalpha is required for RNA polymerase II transcription on chromatin templates. *Nature.* 2001;413(6854):435-8.
109. Pinzone MR, VanBelzen DJ, Weissman S, Bertuccio MP, Cannon L, Venanzi-Rullo E, et al. Longitudinal HIV sequencing reveals reservoir expression leading to decay which is obscured by clonal expansion. *Nature Communications.* 2019;10(1):728.
110. Purcell DF, and Martin MA. Alternative splicing of human immunodeficiency virus type 1 mRNA modulates viral protein expression, replication, and infectivity. *J Virol.* 1993;67(11):6365-78.
111. Dlamini Z, and Hull R. Can the HIV-1 splicing machinery be targeted for drug discovery? *HIV/AIDS - Research and Palliative Care.* 2017;Volume 9:63-75.
112. Pinzone MR, VanBelzen DJ, Weissman S, Bertuccio MP, Cannon L, Venanzi-Rullo E, et al. Longitudinal HIV sequencing reveals reservoir expression leading to decay which is obscured by clonal expansion. *Nat Commun.* 2019;10(1):728.

113. Cesana D, Santoni de Sio FR, Rudilosso L, Gallina P, Calabria A, Beretta S, et al. HIV-1-mediated insertional activation of STAT5B and BACH2 trigger viral reservoir in T regulatory cells. *Nat Commun.* 2017;8(1):498.
114. Ho YC, Shan L, Hosmane NN, Wang J, Laskey SB, Rosenbloom DI, et al. Replication-competent noninduced proviruses in the latent reservoir increase barrier to HIV-1 cure. *Cell.* 2013;155(3):540-51.
115. Massanella M, Gianella S, Lada SM, Richman DD, and Strain MC. Quantification of Total and 2-LTR (Long terminal repeat) HIV DNA, HIV RNA and Herpesvirus DNA in PBMCs. *Bio Protoc.* 2015;5(11):e1492.
116. Merico D, Isserlin R, Stueker O, Emili A, and Bader GD. Enrichment map: a network-based method for gene-set enrichment visualization and interpretation. *PLoS One.* 2010;5(11):e13984.

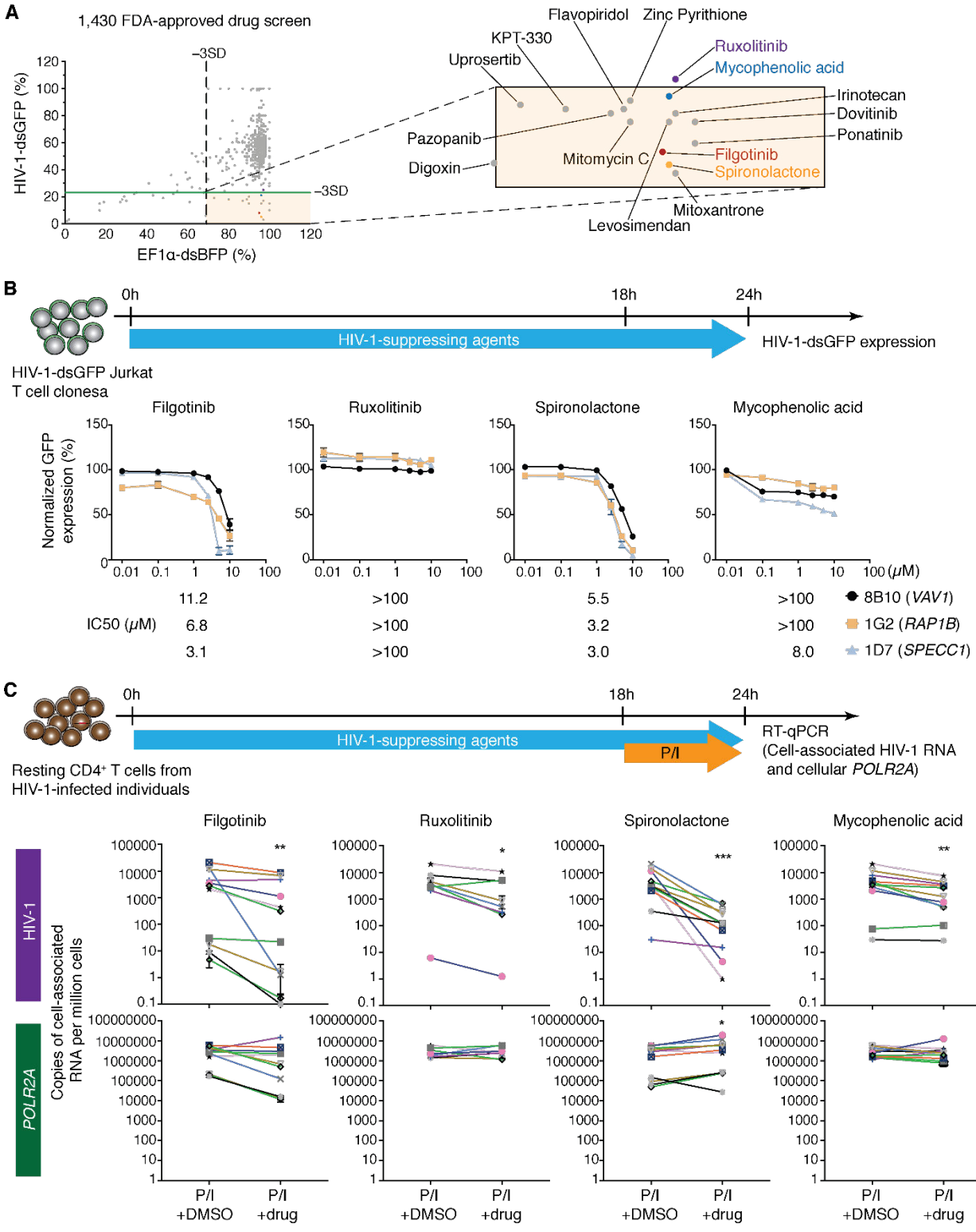
A
1,430 FDA-approved drug screen
HIV-1-dsGFP (%)
EF1α-dsBFP (%)
−3SD
−3SD
Flavopiridol
Zinc Pyrithione
KPT-330
Uprosertib
Ruxolitinib
Mycophenolic acid
Irinotecan
Dovitinib
Ponatinib
Pazopanib
Digoxin
Mitomycin C
Filgotinib
Spironolactone
Mitoxantrone
Levosimendan
B
0h
18h
24h
HIV-1-suppressing agents
HIV-1-dsGFP expression
HIV-1-dsGFP Jurkat
T cell clonesa
Filgotinib
Ruxolitinib
Spironolactone
Mycophenolic acid
Normalized GFP expression (%)
(μM)
IC50 (μM)
11.2
6.8
3.1
>100
>100
>100
5.5
3.2
3.0
>100
>100
8.0
8B10 (VAV1)
1G2 (RAP1B)
1D7 (SPECC1)
C
0h
18h
24h
HIV-1-suppressing agents
P/I
RT-qPCR
(Cell-associated HIV-1 RNA
and cellular POLR2A)
Resting CD4+ T cells from
HIV-1-infected individuals
Filgotinib
Ruxolitinib
Spironolactone
Mycophenolic acid
HIV-1
POLR2A
Copies of cell-associated
RNA per million cells
P/I
+DMSO
P/I
+drug

Figure 1. A dual reporter screen identified HIV-1-suppressing agents. (**A**) Screening of 1,430 small molecule compounds from an FDA-approved drug library identified 16 HIV-1-suppressing agents in dual color Jurkat clone 1B6-du. (**B**) Dose response curves of candidate HIV-1-suppressing agents in three cell line models. HIV-1-dsGFP expression levels were normalized to the levels in DMSO-treated samples. Error bars represent standard errors from quadruplicates. (**C**) Cell-associated RNA levels of polyadenylated HIV-1 and a housekeeping gene *POLR2A* in $CD4^+$ T cells from virally suppressed HIV-1-infected individuals upon treatment with HIV-1-suppressing agents (10 μM for 24 hours) and PMA/ionomycin challenge (for 6 hours) in the presence of ART (1 μM of tenofovir and 10 μM enfuvirtide). Each color represents samples from an HIV-1-infected individual. ds, destabilized protein through PEST sequence-mediated ubiquitination, giving the fluorescent proteins a half-life of two hours (42) for real-time reflection of HIV-1-dsGFP and EF1α-dsBFP expression levels. GFP, green fluorescent protein. BFP, blue fluorescent protein. NLS, nuclear localization signal. P/I, PMA/ionomycin. DMSO, dimethylsulfoxide. *, $p < 0.05$; **, $p < 0.01$; ***, $p < 0.001$ by two-tailed Wilcoxon rank-sum test.

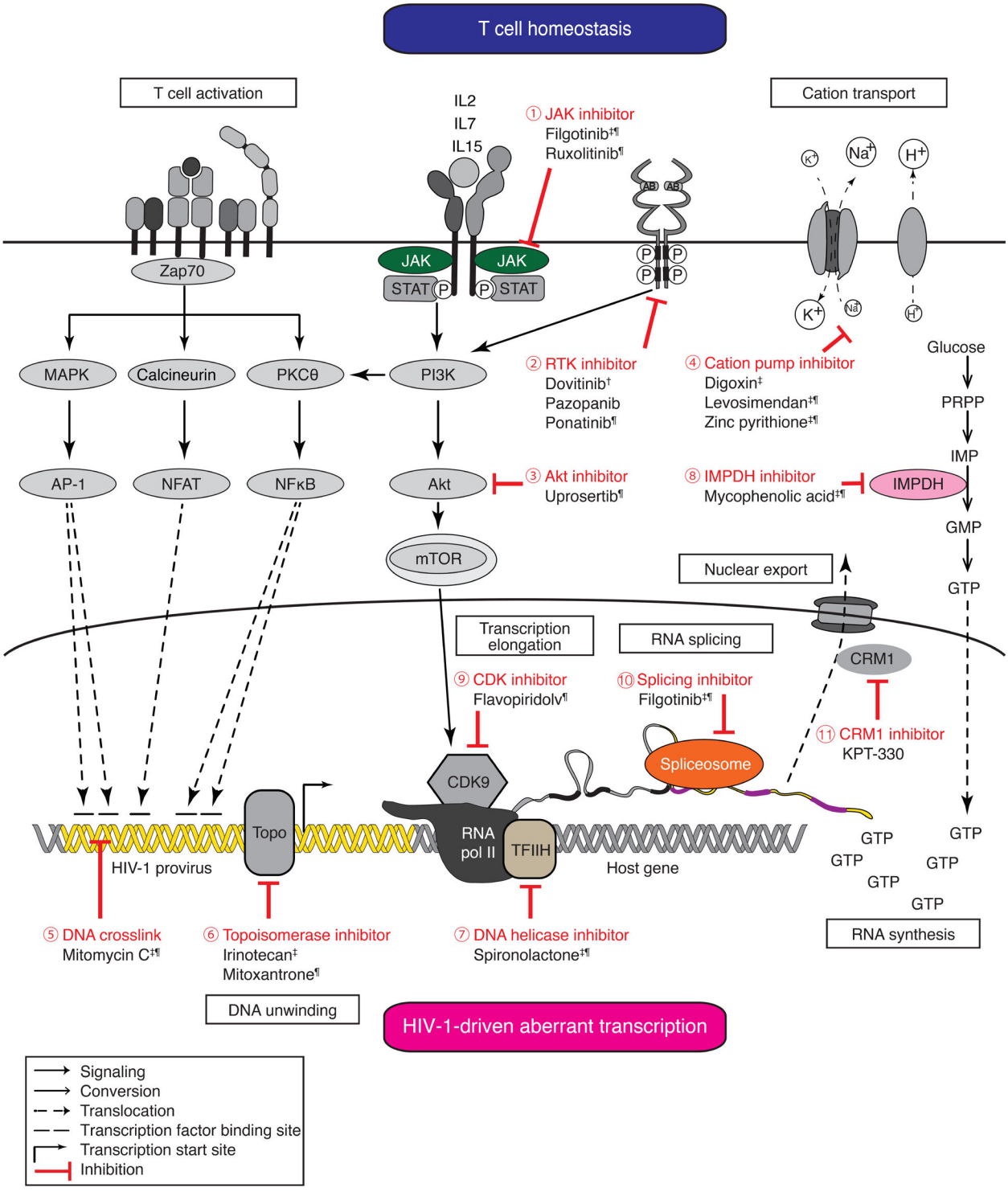

Figure 2. Therapeutic targets of HIV-1 reactivation. A high-throughput drug screen identified 11 cellular pathways critical for HIV-1 transcription after HIV-1 integration. †, preferential HIV-1 suppression in one additional cell line. ‡, HIV-1 suppression in two additional cell lines. ¶, HIV-1 suppression in CD4⁺ T cells from virally suppressed HIV-1-infected individuals.

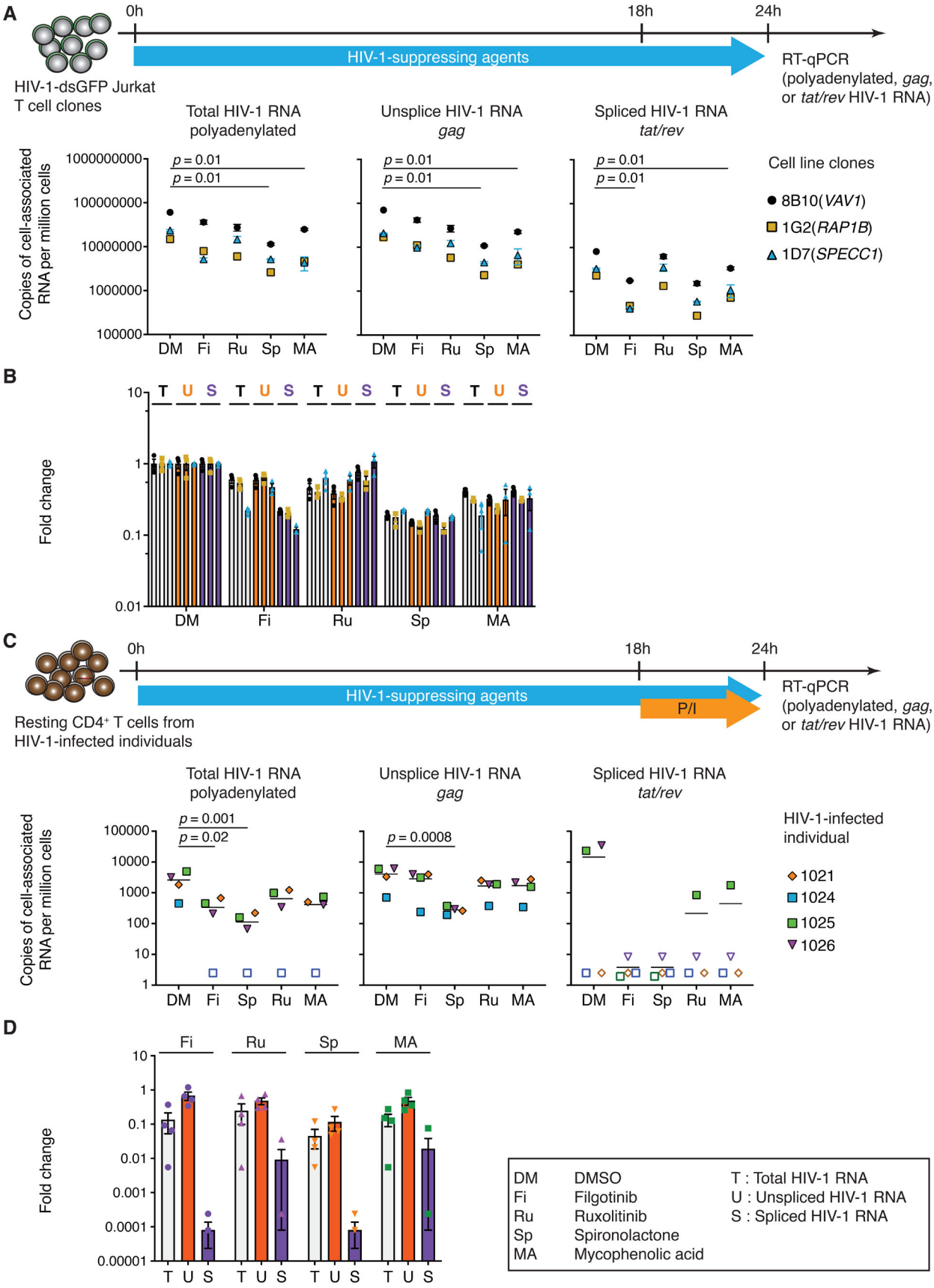
A
0h
18h
24h
HIV-1-suppressing agents
RT-qPCR
(polyadenylated, gag,
or tat/rev HIV-1 RNA)
HIV-1-dsGFP Jurkat
T cell clones
Total HIV-1 RNA
polyadenylated
Unsplice HIV-1 RNA
gag
Spliced HIV-1 RNA
tat/rev
Copies of cell-associated
RNA per million cells
p = 0.01
p = 0.01
DM Fi Ru Sp MA
Cell line clones
8B10(VAV1)
1G2(RAP1B)
1D7(SPECC1)
B
Fold change
T U S
DM Fi Ru Sp MA
C
0h
18h
24h
HIV-1-suppressing agents
P/I
RT-qPCR
(polyadenylated, gag,
or tat/rev HIV-1 RNA)
Resting CD4+ T cells from
HIV-1-infected individuals
Total HIV-1 RNA
polyadenylated
Unsplice HIV-1 RNA
gag
Spliced HIV-1 RNA
tat/rev
p = 0.001
p = 0.02
p = 0.0008
DM Fi Sp Ru MA
HIV-1-infected
individual
1021
1024
1025
1026
D
Fi Ru Sp MA
Fold change
T U S
DM DMSO
Fi Filgotinib
Ru Ruxolitinib
Sp Spironolactone
MA Mycophenolic acid
T : Total HIV-1 RNA
U : Unspliced HIV-1 RNA
S : Spliced HIV-1 RNA

Figure 3. HIV-1-suppressing agents reduce different levels of spliced and unspliced HIV-1 RNA transcription. Cell-associated RNA levels (**A, C**) and fold inhibition (**B, D**) of total (polyadenylated)(68), unspliced (*gag*)(69), and spliced (*tat/rev*)(115) HIV-1 RNA in three HIV-1-dsGFP-Jurkat clones (**A, B**) and $CD4^+$ T cells from virally suppressed, HIV-1-infectd individuals (**C, D**) were measured by RT-qPCR. Cells were treated with with HIV-1-suppressing agents (10 μM for 24 hours). In clinical samples (**C, D**), aliquots of 1 million cells were treated with PMA/ionomycin challenge (for 6 hours) in the presence of ART (1 μM of tenofovir and 10 μM enfuvirtide). *p*-values were calculated by nonparametric ANOVA Friedman's test (two-tailed) with uncorrected Dunn's test for comparison between each treatment to DMSO control. Error bars represent standard errors from quadruplicates. DM, DMSO; Fi, JAK1 inhibitor filgotinib; Ru, JAK1/2 inhibitor ruxolitinib; Sp, DNA helicase inhibitor spironolactone; MA, IMPDH inhibitor mycophenolic acid.

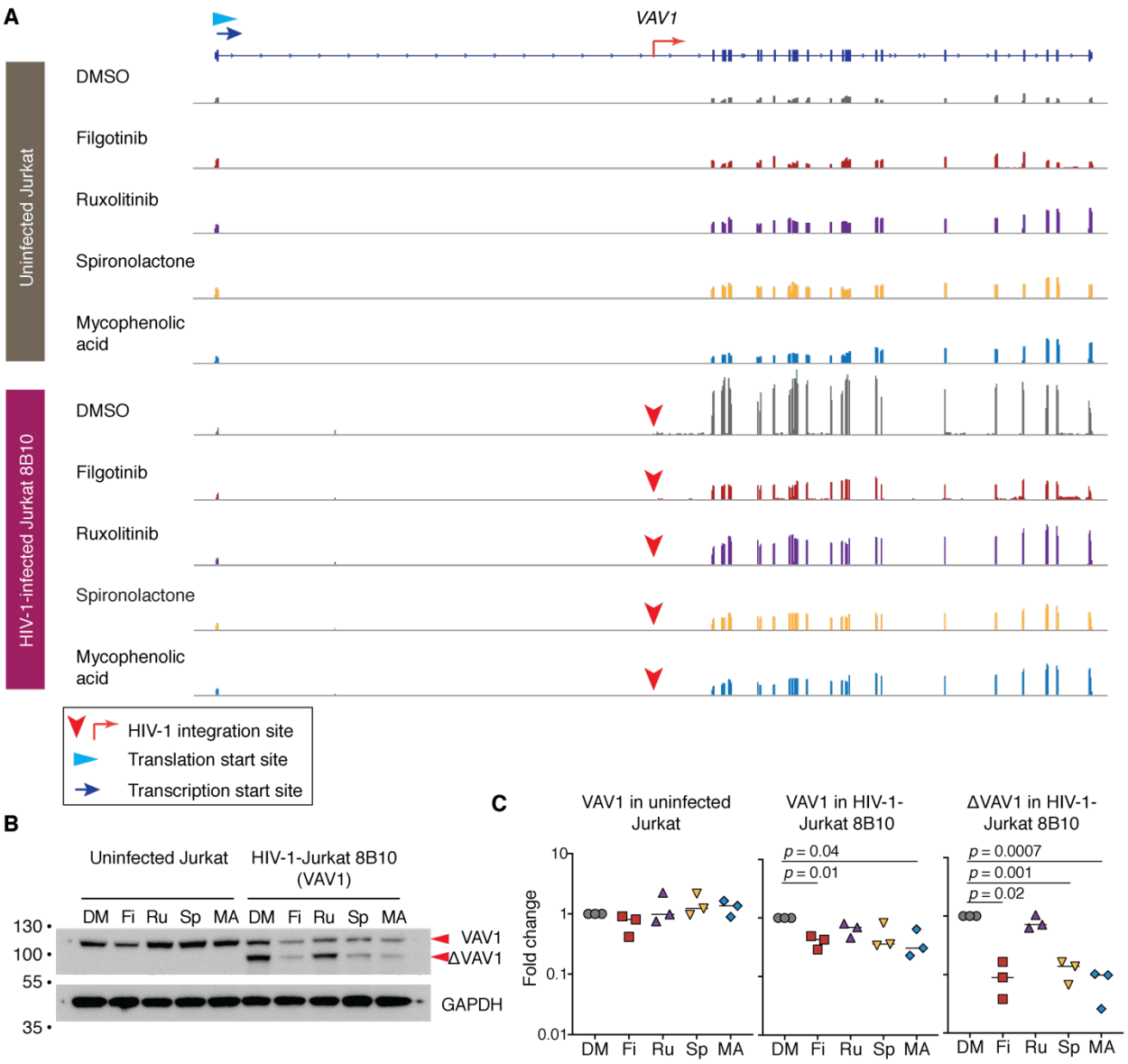

Figure 4. HIV-1-suppressing agents reduce HIV-1-driven aberrant host gene transcription at the integration site. (**A**) Normalized transcriptional landscape using first exon at the HIV-1 integration site (proto-oncogene *VAV1*) in the HIV-1-Jurkat clone 8B10 treated with HIV-1-suppressing agents (10 μM) for 24 hours. HIV-1 integration into *VAV1* has been previously reported in CD4$^+$ T cells from virally suppressed HIV-1-infected individuals (72). Red arrowhead, HIV-1 integration site mapped by inverse PCR (58). (**B**) Western blot of VAV1 protein expression in HIV-1-infected Jurkat clone 8B10 treated with HIV-1-suppressing agents. (**C**) Relative quantification of intact VAV1 and truncated VAV1 expression to DMSO treatment

normalized to GAPDH in triplicates. DM, DMSO; Fi, filgotinib; Ru, ruxolitinib; Sp, spironolactone; MA, mycophenolic acid. *p*-value was calculated with one-way ANOVA with Fisher's LSD test for comparison between each treatment to DMSO control.

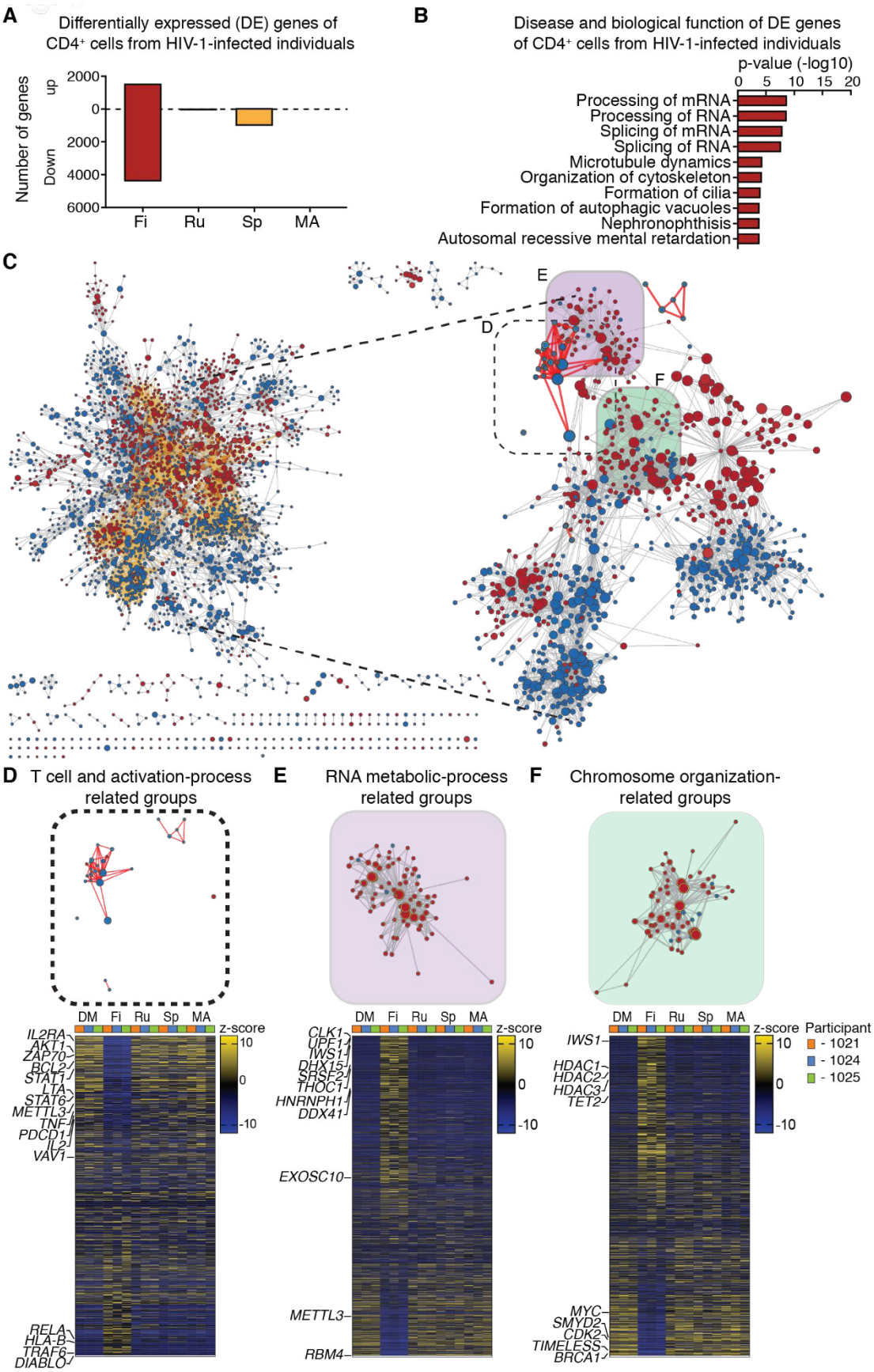
A
Differentially expressed (DE) genes of CD4+ cells from HIV-1-infected individuals
Number of genes
up
Down
2000
0
2000
4000
6000
Fi
Ru
Sp
MA
B
Disease and biological function of DE genes of CD4+ cells from HIV-1-infected individuals
p-value (-log10)
0 5 10 15 20
Processing of mRNA
Processing of RNA
Splicing of mRNA
Splicing of RNA
Microtubule dynamics
Organization of cytoskeleton
Formation of cilia
Formation of autophagic vacuoles
Nephronophthisis
Autosomal recessive mental retardation
C
D
E
F
D T cell and activation-process related groups
E RNA metabolic-process related groups
F Chromosome organization-related groups
DM Fi Ru Sp MA
z-score
10
0
-10
IL2RA
AKT1
ZAP70
BCL2
STAT1
LTA
STAT6
METTL3
TNF
PDCD1
IL2
VAV1
RELA
HLA-B
TRAF6
DIABLO
CLK1
UPF1
IWS1
DHX15
SRSF2
THOC1
HNRNPH1
DDX41
EXOSC10
METTL3
RBM4
IWS1
HDAC1
HDAC2
HDAC3
TET2
MYC
SMYD2
CDK2
TIMELESS
BRCA1
Participant
- 1021
- 1024
- 1025

Figure 5. Pathway enrichment analysis of CD4$^+$ T cell from virally suppressed, HIV-1-infected individuals treated with HIV-1-suppressing agents ex vivo. (**A**) Differential gene expression analysis of CD4$^+$ T cells from three virally suppressed, HIV-1-infected individuals (#1021, #1024, and #1025) treated with 10 μM HIV-1-suppressing agents for 24 hours in the presence of ART (1 μM of tenofovir and 10 μM enfuvirtide). (**B**) Disease and biological function pathway analysis of differential expressed genes using ingenuity pathway analysis (IPA). (**C**) Results of gene set enrichment analysis (GSEA)(77) with gene ontology (GO) gene sets visualized by EnrichmentMap in Cytoscape (116). Each node represents one GO gene set in GSEA Molecular Signature Database (MSigDB) that is significantly enriched (false discovery rate (FDR) < 0.25). The size of the node represents the number of genes in each gene set. Color red represents a positive enrichment score and color blue represents a negative enrichment score. The edge (connected lines between nodes) represents the degree of gene overlap between nodes. The cutoff of overlap coefficient is 1. We identified the most enriched pathways from top 17 nodes with >50 interactions each. The expression levels of T cell activation-related gene sets (**D**), RNA metabolic process-related genes (**E**) and chromatin organization-related genes (**F**) were analyzed using CD4$^+$ T cells from three virally suppressed HIV-1-infected individuals. DM, DMSO; Fi, filgotinib; Ru, ruxolitinib; Sp, spironolactone; MA, mycophenolic acid.

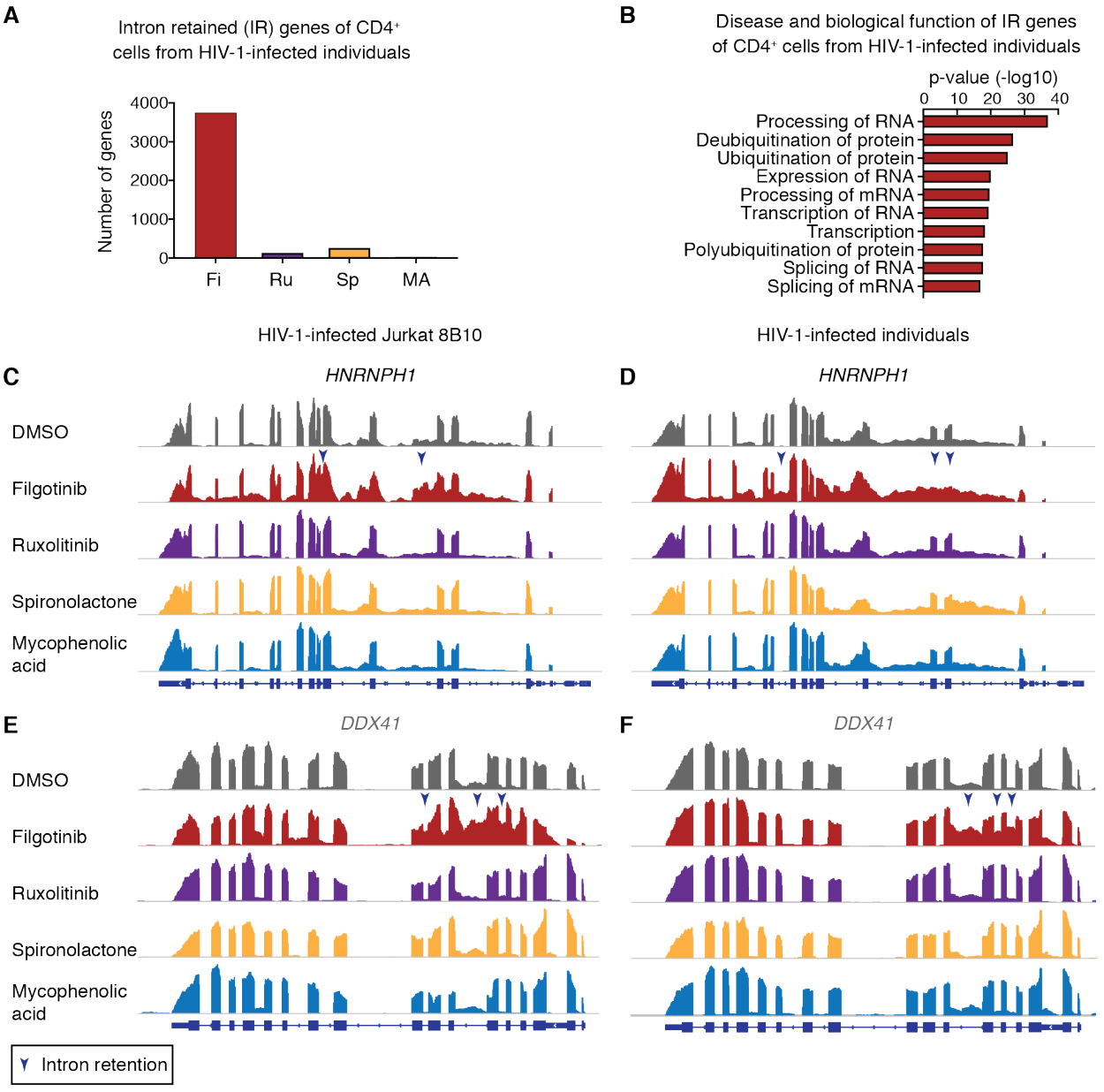
A
Intron retained (IR) genes of CD4+ cells from HIV-1-infected individuals
Number of genes
4000
3000
2000
1000
0
Fi
Ru
Sp
MA
B
Disease and biological function of IR genes of CD4+ cells from HIV-1-infected individuals
p-value (-log10)
0 10 20 30 40
Processing of RNA
Deubiquitination of protein
Ubiquitination of protein
Expression of RNA
Processing of mRNA
Transcription of RNA
Transcription
Polyubiquitination of protein
Splicing of RNA
Splicing of mRNA
HIV-1-infected Jurkat 8B10
HIV-1-infected individuals
C
HNRNPH1
D
HNRNPH1
DMSO
Filgotinib
Ruxolitinib
Spironolactone
Mycophenolic acid
E
DDX41
F
DDX41
Intron retention
G
DM Fi Ru Sp MA
100
70
55
35
DDX41
HNRNPH1
GAPDH

Figure 6. Filgotinib induces intron retention in RNA processing-related genes in both HIV-1-infected Jurkat clone 8B10 and CD4$^+$ T cell from virally suppressed, HIV-1-infected individuals. (**A**) The number of intron-retained genes identified by IRFinder (78) in CD4$^+$ T cells treated with HIV-1-suppressing agents using samples described in Figure 5. CD4$^+$ T cells were obtained from three virally suppressed, HIV-1-infected individuals (#1021, #1024, and #1025) treated with 10 μM HIV-1-suppressing agents for 24 hours in the presence of ART (1 μM of tenofovir and 10 μM enfuvirtide). Intron-retained regions with significant increased ratio ($p <$ 0.05, unequal variances *t*-test) were reported. (**B**) Disease and biological function pathway analysis of intron-retained genes using IPA in CD4$^+$ T cells from three virally suppressed, HIV-1-infected individuals treated with filgotinib. Integrative genome viewer (IGV) plots of representative RNA landscape of *HNRNPH1* and *DDX41* demonstrate intron retention in these genes (blue arrows) in HIV-dsGFP Jurkat clone 8B10 (**C, E**) and in CD4$^+$ T cells from virally suppressed, HIV-1-infected individuals (**D, F**). (**G**) Western blot of intron-retained genes HNRNPH1 and DDX41 in HIV-1-infected Jurak 8B10 cells treated with HIV-1-suppressing agents. DM, DMSO; Fi, filgotinib; Ru, ruxolitinib; Sp, spironolactone; MA, mycophenolic acid.

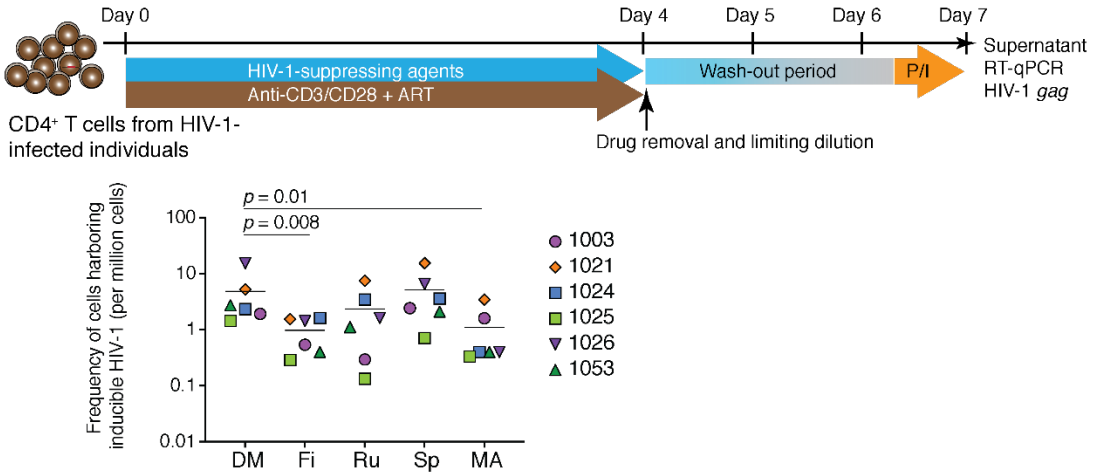

Figure 7. HIV-1-suppressing agents reduce the frequency of cells harboring inducible HIV-1. CD4⁺ T cells from 6 virally suppressed, HIV-1-infected individuals were activated with anti-CD3/CD28 antibodies for four days in the presence of HIV-1-suppressing agents (10 μM) and ART (1 μM tenofovir and 10 μM enfuvirtide) to allow cellular proliferation without new rounds of infection. Cells were plated at limiting dilution (200,000 cells per well) to calculate the frequency of cells harboring inducible HIV-1. After two days allowing wash-out of the HIV-1-suppressing agents, cells were stimulated with PMA/ionomycin to induce HIV-1 RNA expression. The use of inducible HIV-1 RNA assay by measuring supernatant HIV-1 RNA allows a wide dynamic range to calculate the frequency of cells harboring inducible HIV-1. *p*-values were calculated by nonparametric ANOVA Friedman's test (two-tailed) with uncorrected Dunn's test for comparison between each treatment to DMSO control. DM, DMSO; Fi, filgotinib; Ru, ruxolitinib; Sp, spironolactone; MA, mycophenolic acid.

Graphical abstract

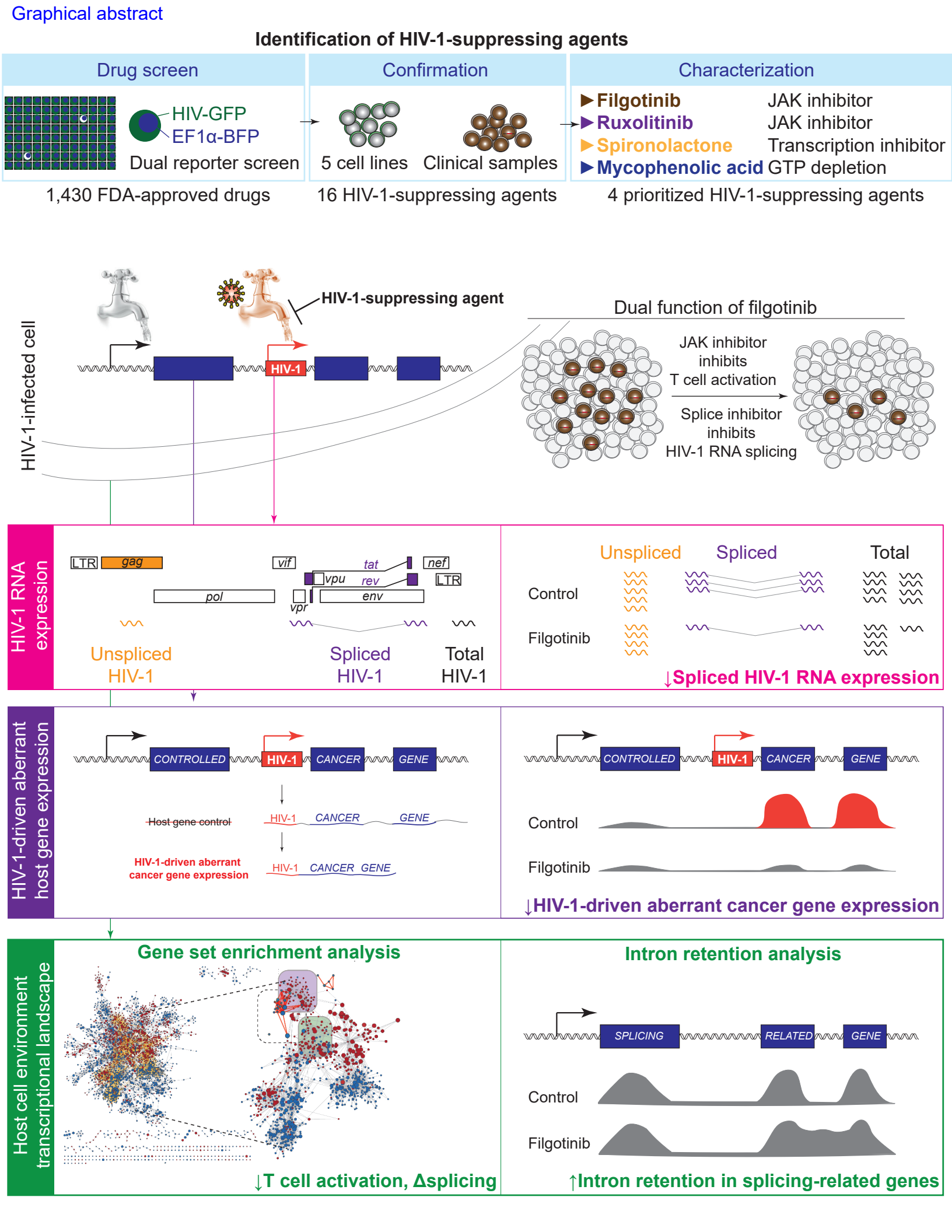

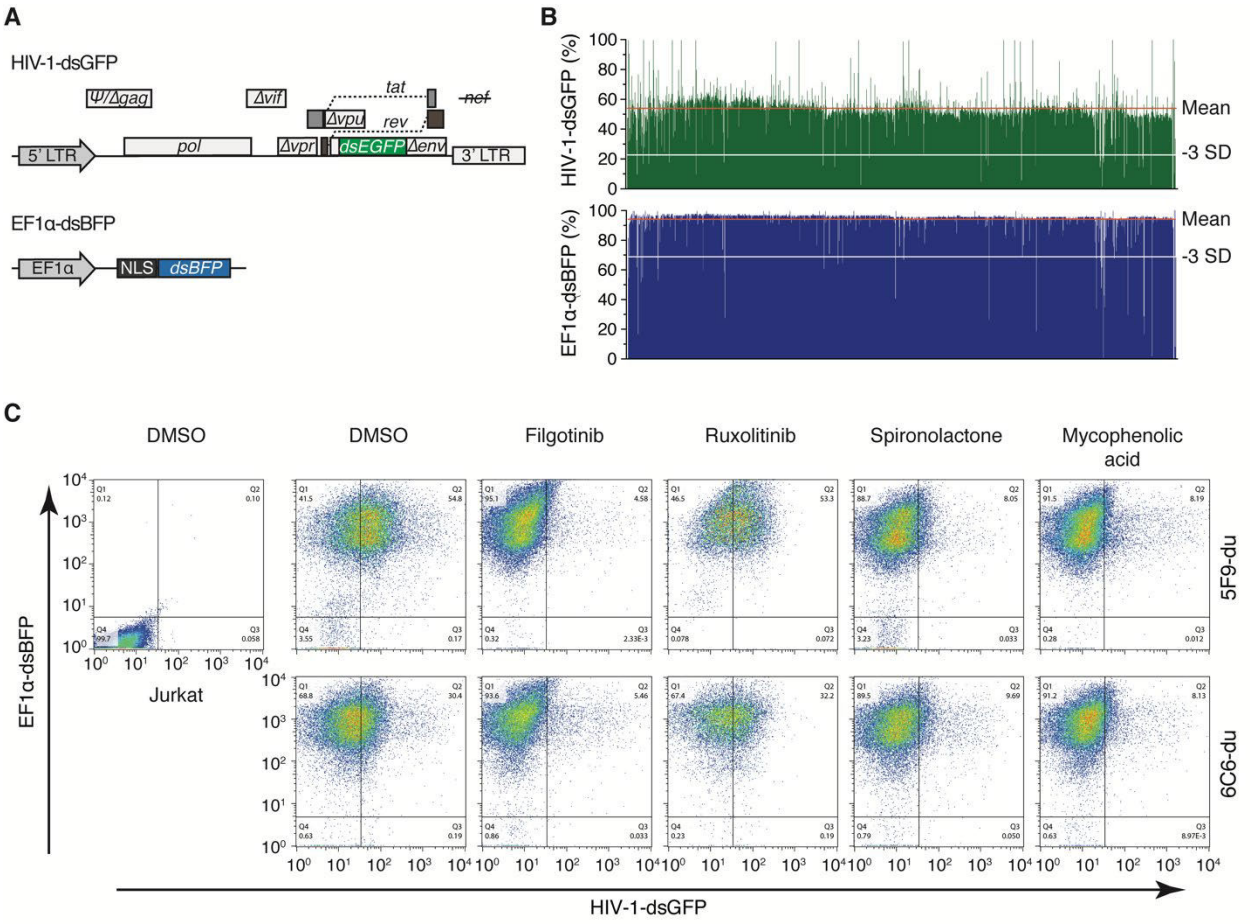

Figure S1. An FDA-approved small molecule compound library screen identified HIV-1-suppressing agents. (**A**) Scheme of the lentiviral reporter constructs. The HIV-1-dsGFP reporter has an NL4-3-EGFP-derived full-length HIV-1 provirus which preserves HIV-1 splice sites and cis-acting elements such as TAR and RRE. Six inactivating mutations were introduced into *gag*, *vif*, *vpr*, *vpu* with trucated *nef* and deleted *env* to reduce cellular toxicity (44). Both dsGFP and dsBFP are targeted for rapid degradation through the PEST sequence, resulting in a short half-life of 2 hours (*44*) and thus a real-time reflection of HIV-1-driven dsGFP and EF1α-driven dsBFP expression. We separated dsGFP and dsBFP in different cellular compartments to avoid fluorescent resonant energy transfer (FRET) between dsBFP and dsGFP: the dsGFP is targeted into the endoplasmic reticulum through the signal peptide leader sequence, while the

dsBFP is targeted into the nucleus by a nuclear localization signal (NLS). (**B**) A small molecule compound library of 1,430 FDA-approved drugs (10 μM) were screened in 96-well plates with dual color Jurkat clone 1B6-du (integration site *ITGAE*) for 24 hours. In each 96-well plate, four wells of flavopiridol served as positive controls and four wells of DMSO served as negative controls. Drugs which can suppress HIV-1-dsGFP expression three standard deviations below mean without reducing EF1α-driven dsBFP expression for more than three standard deviations below mean were considered as candidate HIV-1-suppressing agents for further evaluation. (**C**) Representative flow cytometry plots of dual reporter HIV-1-infected Jurkat clones 5F9-du and 6C6-du treated with 10 μM HIV-1-suppressing agents for 24 hours. GFP, green fluorescent protein. BFP, blue fluorescent protein. NLS, nuclear localization signal.

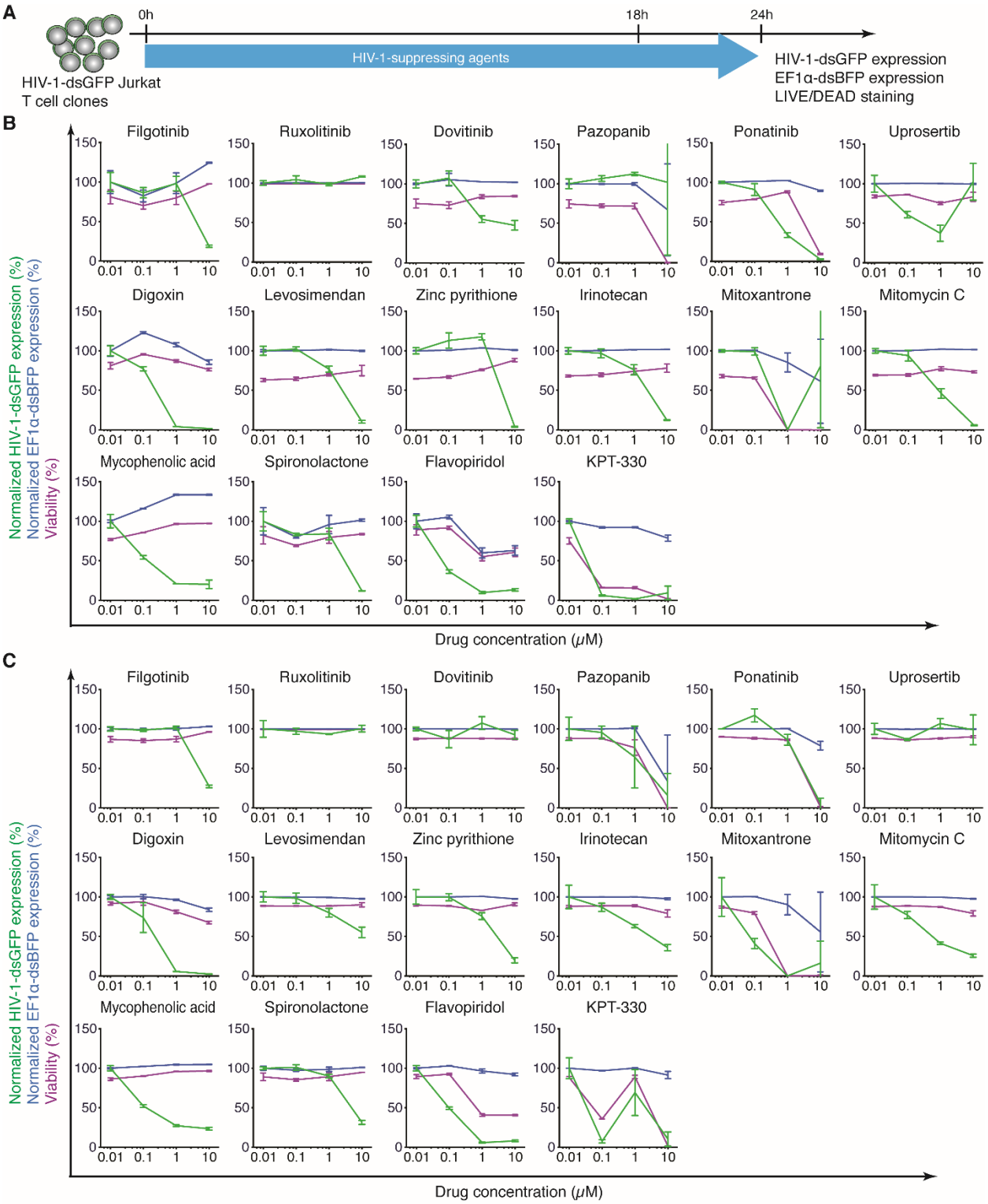
A
0h
18h
24h
HIV-1-suppressing agents
HIV-1-dsGFP Jurkat
T cell clones
HIV-1-dsGFP expression
EF1α-dsBFP expression
LIVE/DEAD staining
B
C
Filgotinib
Ruxolitinib
Dovitinib
Pazopanib
Ponatinib
Uprosertib
Digoxin
Levosimendan
Zinc pyrithione
Irinotecan
Mitoxantrone
Mitomycin C
Mycophenolic acid
Spironolactone
Flavopiridol
KPT-330
Normalized HIV-1-dsGFP expression (%)
Normalized EF1α-dsBFP expression (%)
Viability (%)
Drug concentration (μM)

Figure S2. Dose response curves and viability measurement using dual-color HIV-1-infected Jurkat clones treated with HIV-1-suppressing agents. (**A**) Schematic presentation of the experimental design. (**B–C**) Dose response curves of HIV-dsGFP, EF1α-dsBFP, and viability of (**B**) HIV-1-infected Jurkat 5F9-du (integration site *INPPL1*) and (**C**) HIV-1-infected Jurkat 6C6-du (integration site *PLGLB1*) for 24 hours. The expression levels were normalized to that of DMSO-treated controls.

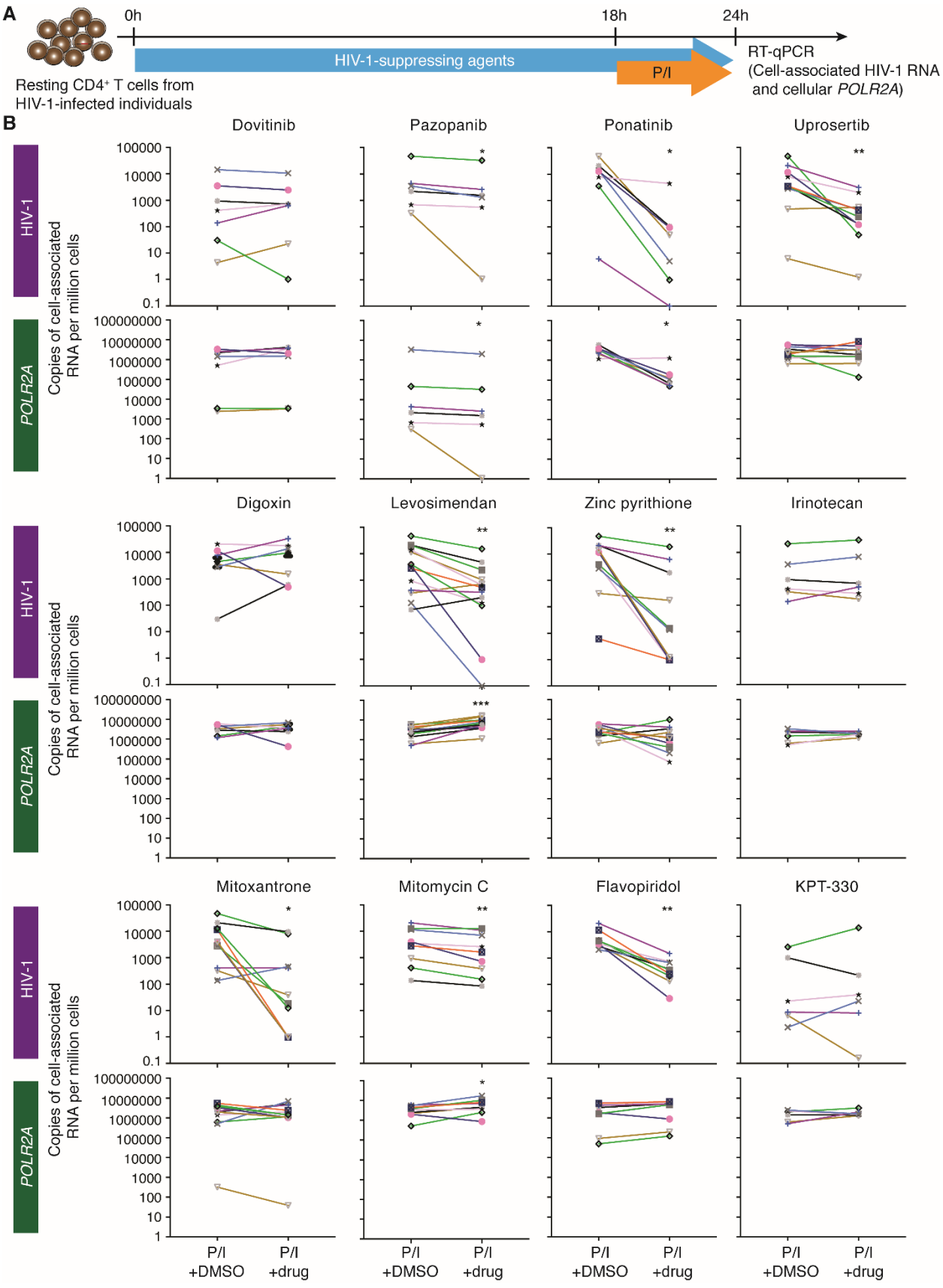
A
0h
18h
24h
HIV-1-suppressing agents
P/I
RT-qPCR
(Cell-associated HIV-1 RNA
and cellular POLR2A)
Resting CD4+ T cells from
HIV-1-infected individuals
B
Dovitinib
Pazopanib
Ponatinib
Uprosertib
Digoxin
Levosimendan
Zinc pyrithione
Irinotecan
Mitoxantrone
Mitomycin C
Flavopiridol
KPT-330
HIV-1
POLR2A
Copies of cell-associated
RNA per million cells
P/I
+DMSO
P/I
+drug

Figure S3. Cell-associated RNA levels of polyadenylated HIV-1 and a housekeeping gene *POLR2A* of candidate HIV-1-suppressing agents. (**A**) Schematic representation of the experimental design. (**B**) Cell-associated RNA levels of polyadenylated HIV-1 and a housekeeping gene *POLR2A* in $CD4^+$ T cells from virally suppressed, HIV-1-infected individuals upon treatment with HIV-1-suppressing agents (10 μM) for 24 hours and PMA/ionomycin challenge during the final 6 hours in the presence of ART (1 μM of tenofovir and 10 μM enfuvirtide). Each color represents one HIV-1-infected individual. P/I, PMA/ionomycin. *, $p < 0.05$; **, $p < 0.01$; ***, $p < 0.001$ by two-tailed Wilcoxon ranksum test.

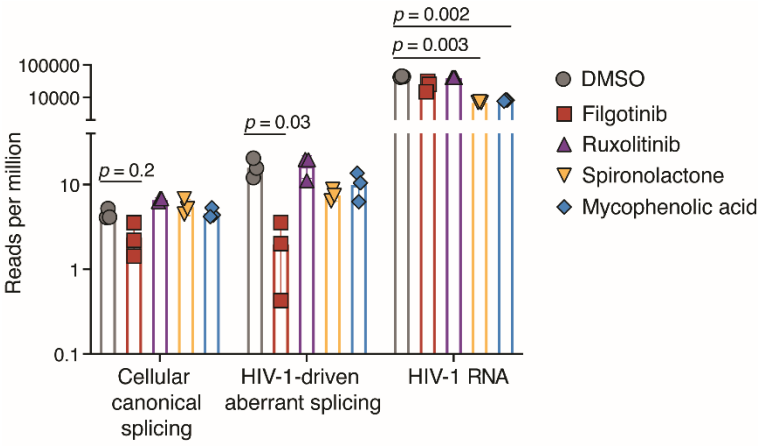

Figure S4. Effect of HIV-1-suppressing agents on host, HIV-1-to-host and HIV-1 RNA splicing in HIV-1-infected Jurkat clone 8B10. To examine the effect of HIV-1-suppressing agents on RNA splicing, we examined cellular canonical splicing (from *VAV1* exon 1 to *VAV1* exon 2), HIV-1-to-host aberrant splicing (from HIV-1 major splice donor site to *VAV1* exon 2), and HIV-1 RNA expression (total HIV-1 RNA). Reads were normalized to total mapped reads and presented as reads per million total reads. Analysis was performed using the same triplicated RNA-seq data for each treatment as described in Figure 4. *p*-values were calculated using repeated measures two-way ANOVA with Geisser-Greenhouse correction and *post hoc* analysis with Dunnett's multiple comparisons test.

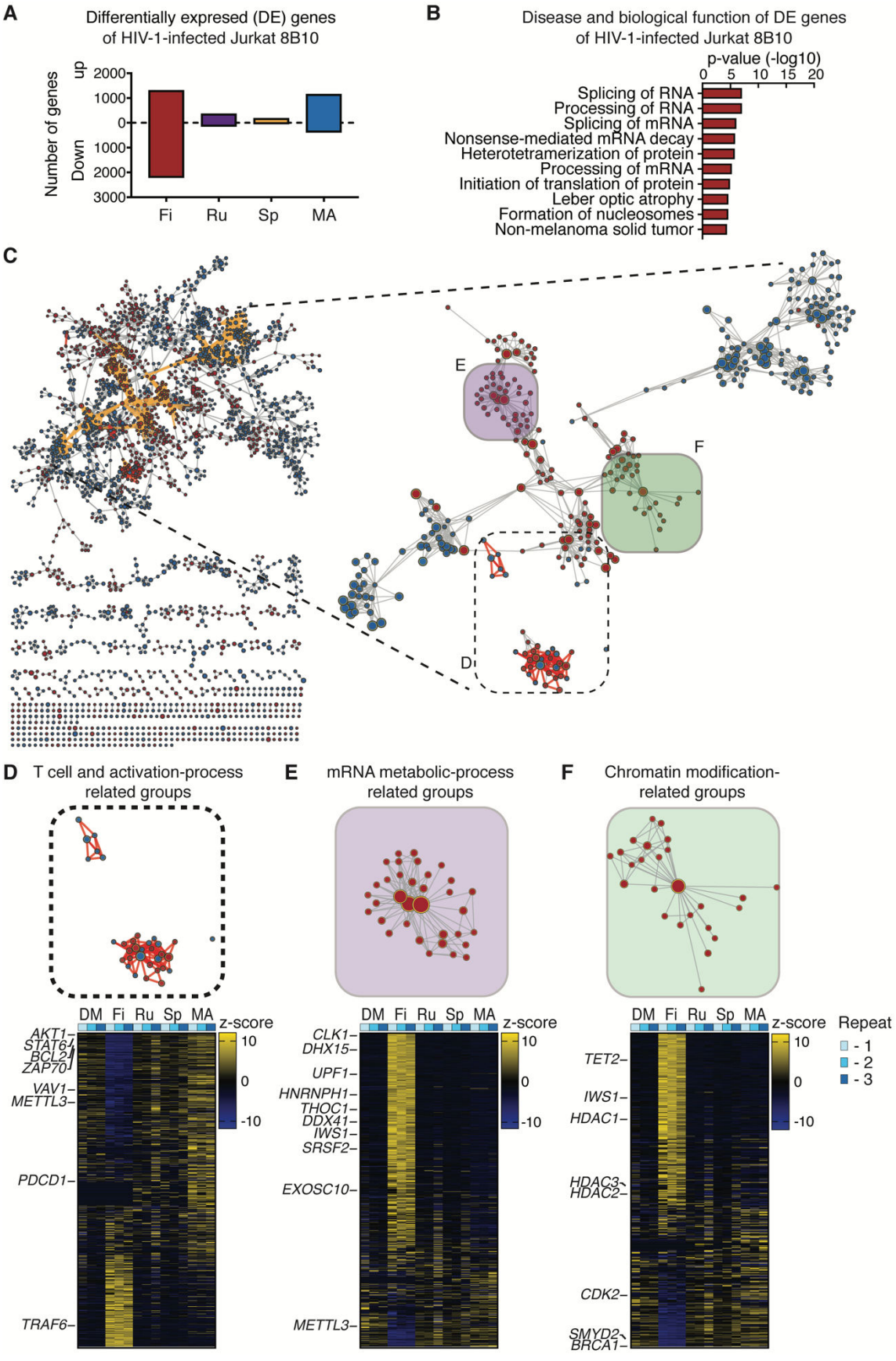
A
Differentially expresed (DE) genes
of HIV-1-infected Jurkat 8B10
Number of genes
up
Down
2000
1000
0
1000
2000
3000
Fi
Ru
Sp
MA
B
Disease and biological function of DE genes
of HIV-1-infected Jurkat 8B10
p-value (-log10)
0
5
10
15
20
Splicing of RNA
Processing of RNA
Splicing of mRNA
Nonsense-mediated mRNA decay
Heterotetramerization of protein
Processing of mRNA
Initiation of translation of protein
Leber optic atrophy
Formation of nucleosomes
Non-melanoma solid tumor
C
E
F
D
D
T cell and activation-process
related groups
E
mRNA metabolic-process
related groups
F
Chromatin modification-
related groups
DM
Fi
Ru
Sp
MA
z-score
10
0
-10
AKT1
STAT6
BCL2
ZAP70
VAV1
METTL3
PDCD1
TRAF6
CLK1
DHX15
UPF1
HNRNPH1
THOC1
DDX41
IWS1
SRSF2
EXOSC10
METTL3
TET2
IWS1
HDAC1
HDAC3
HDAC2
CDK2
SMYD2
BRCA1
Repeat
- 1
- 2
- 3

Figure S5. Pathway enrichment analysis of HIV-1-infected Jurkat clone 8B10 treated with HIV-1-suppressing agents. (**A**) Differential gene expression analysis of HIV-1-infected Jurkat clone 8B10 treated with HIV-1-suppressing agents for 24 hours. (**B**) Disease and biological function pathway analysis of differential expressed genes using ingenuity pathway analysis (IPA). (**C**) Results of gene set enrichment analysis (GSEA)(*67*) with gene ontology (GO) gene sets visualized by EnrichmentMap in Cytoscape (*99*). Each node represents one gene set in GSEA Molecular Signature Database (MSigDB) GO gene sets that is significantly enriched (false discovery rate (FDR) < 0.25). The size of the nodes represents the number of genes in each gene set. Color red represents a positive enrichment score and color blue represents a negative enrichment score. The edge (connected lines between nodes) represents the degree of gene overlap between nodes. The cutoff of overlap coefficient is 1. We identified enriched pathways from the top 14 nodes with >22 interactions each. The expression levels of T cell activation-related gene sets (**D**), RNA metabolic process-related genes (**E**) and chromatin organization-related genes (**F**) in triplicates of HIV-1-infecte Jurkat 8B10. All analyses were done in triplicates.

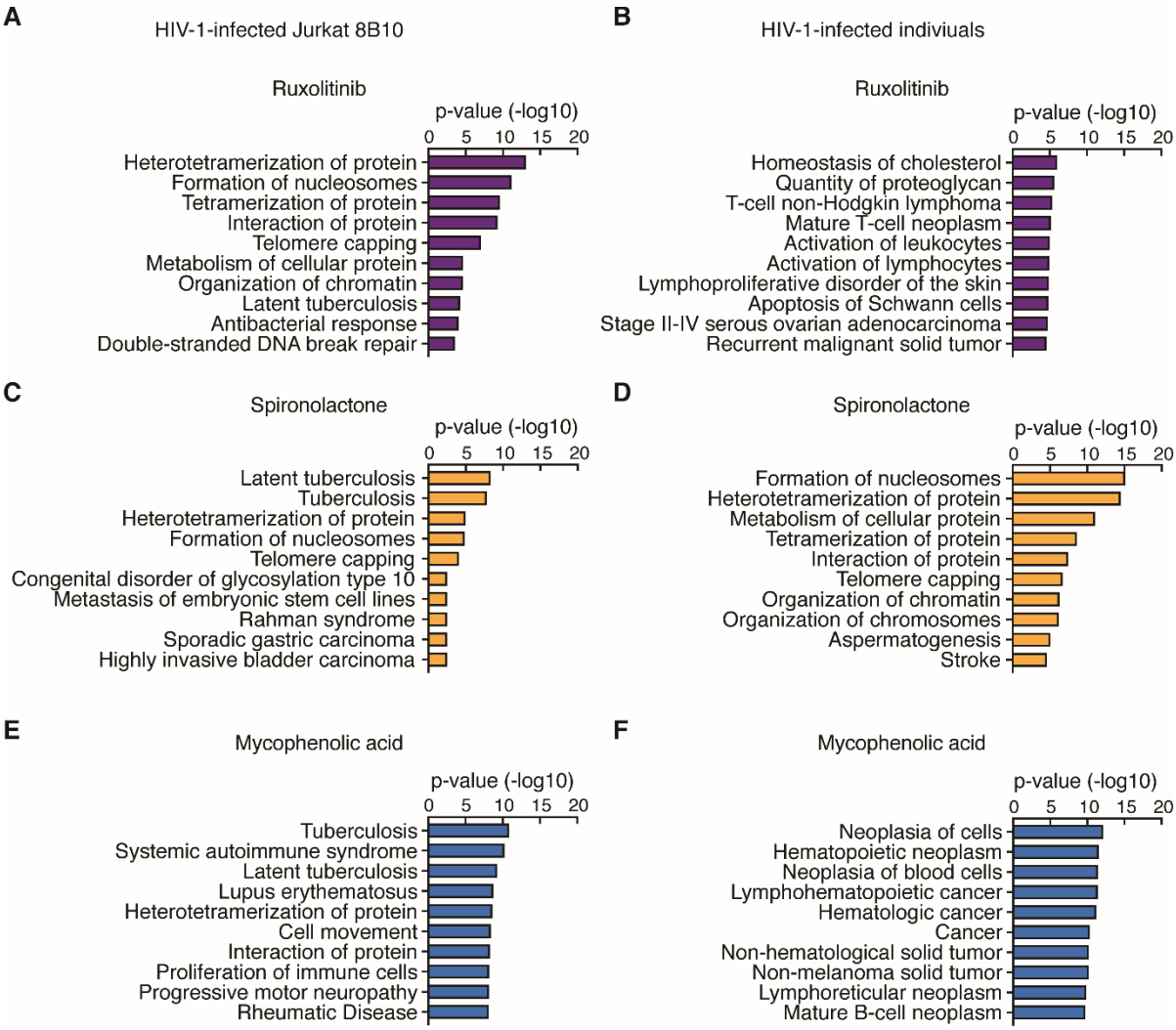

Figure S6. Pathway enrichment analysis using IPA on differentially expressed genes in HIV-infected Jurkat cell clone 8B10 and in CD4⁺ T cells from virally suppressed, HIV-1-infected individuals treated with ruxolitinib, spironolactone and mycophenolic acid. Data reflect triplicates of HIV-1-infected Jurkat 8B10 (**A, C, E**) and CD4⁺ T cells from three virally suppressed, HIV-1-infected individuals (#1021, #1024, and #1025)(**B, D, F**) for 24 hours.

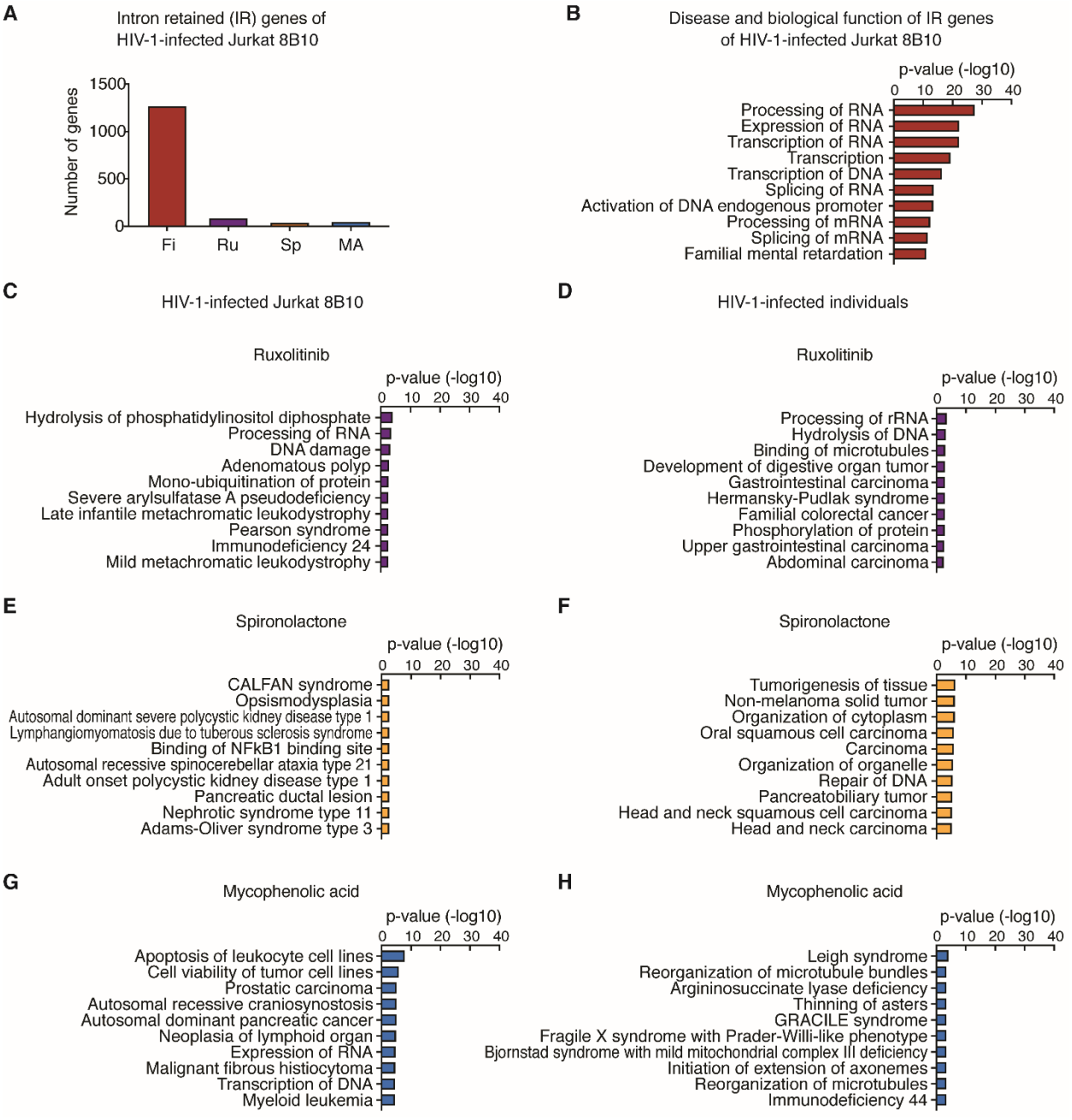

Figure S7. Intron retention analysis of HIV-1-infected Jurkat clone 8B10 and CD4⁺ T cells from virally suppressed, HIV-1-infected individuals treated with ruxolitinib, spironolactone and mycophenolic acid. (**A**) The number of intron-retained genes identified by IRFinder (*84*) in HIV-1-infected Jurkat 8B10 compared with DMSO-treated samples for 24 hours. Intron-retained regions with significantly increased ratio ($p < 0.05$, unequal variances *t*-

test) were reported. (**B**) Disease and biological function pathway analysis of intron retained genes using IPA in HIV-1-infected Jurkat 8B10 treated with filgotinib. Disease and biological functional pathway analysis using IPA demonstrated no significant pathway enrichment in ruxolitinib-treated (**C, D**), spironolactone-treated (**E, F**) and mycophenolic acid-treated (**G, H**) cell line and clinical samples (#1021, #1024, and #1025).

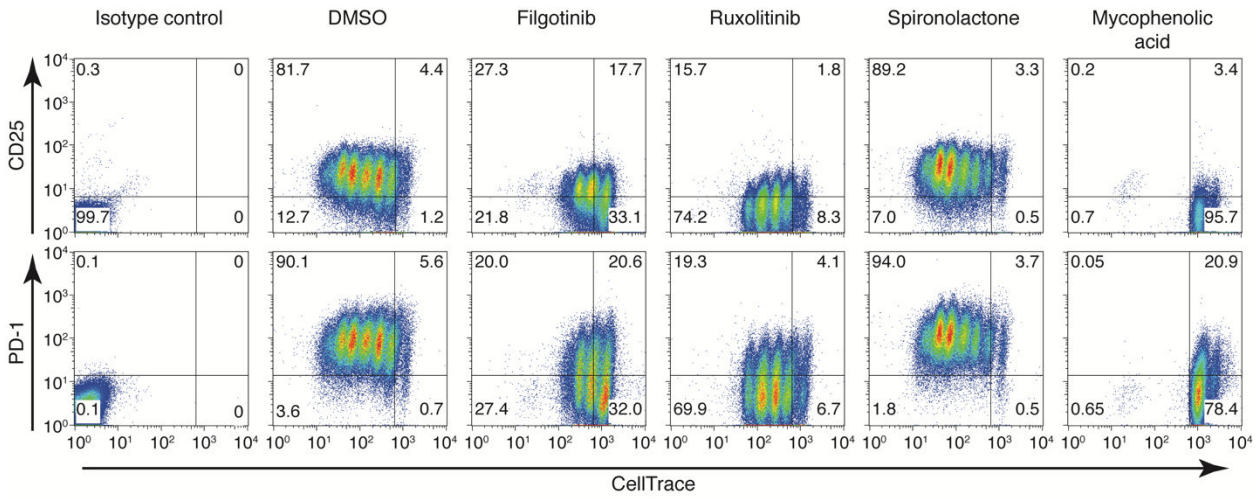

Figure S8. The effect of HIV-1-suppressing agents on T cell activation and cellular proliferation of CD4$^+$ T cell from virally suppressed, HIV-1-infected individuals. CD4$^+$ T cells from a virally suppressed, HIV-1-infected individuals were stained with CellTrace® dye and treated with anti-CD3/CD28 magnetic beads in the presence of ART and respective HIV-1-suppressing agents for 3 days before flow cytometry analysis.

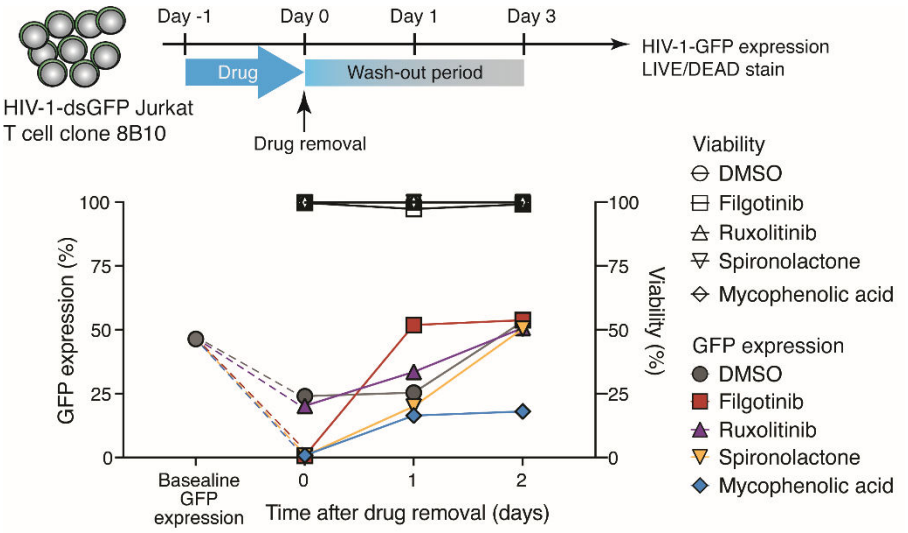

Figure S9. HIV-1-driven GFP expression levels after removal of HIV-1-suppressing agents removal. HIV-1-infected Jurkat clone 8B10 were treated with 10 μM HIV-1-suppressing agents for 24 hours. Agents were removed and GFP expression were measured by flow cytometry. Cells were stained with LIVE/DEAD dye to examine the viability.

Table S1. HIV-1-suppressing agents

HIV-1 suppressing agents	Mechanism of action
T cells activation	
JAK-STAT	
Filgotinib	JAK inhibitor selective for JAK1
Ruxolitinib	JAK inhibitor selective for JAK1/2
Receptor tyrosine kinase	
Dovitinib	Class III, IV and V receptor tyrosine kinase inhibitor
Pazopanib	VEGFR1/2/3, PDGFR, FGFR, c-Kit and c-Fms inhibitor
Ponatinib	Abl, PDGFRα, VEGFR2, FGFR1 and Src inhibitor
AKT	
Uprosertib	Akt inhibitor
Cation transport	
Digoxin	Na^+/K^+ ATPase inhibitor
Levosimendan	Calcium sensitizer
Zinc pyrithione	H^+ pump inhibitor
DNA unwinding process	
Topoisomerase	
Irinotecan	Topoisomerase I inhibitor
Mitoxantrone	Topoisomerase II inhibitor
DNA crosslinking	
Mitomycin C	DNA crosslinker
DNA helicase	
Spironolactone	XPB ATP-dependent DNA helicase (a part of the TFIIH transcription factor complex) inhibitor
RNA synthesis	
De novo guanosine triphosphate synthesis	
Mycophenolic acid	IMPDH inhibitor
Transcription elongation	
Flavopiridol	CDK1, CDK2, CDK4, CDK6, and CDK9 inhibitor
RNA splicing	
Filgotinib	New function identified in this study
RNA nuclear export	
KPT-330	RNA transport inhibitor selective for CRM1

CDK, cyclin-dependent kinase; CRM1, chromosomal maintenance 1; VEGFR, vascular endothelial growth factor Receptor; PDGFR, platelet-derived growth factor receptor; FGFR, fibroblast growth factor receptor; JAK, Janus kinase; IMPDH, Inosine-5′-monophosphate dehydrogenase

Table S2. Characteristics of study participants

ID	Age	Sex	Ethnicity	Current ART	Viral load (copies/ml)	Duration on ART (month)	Duration of undetectable viral load (month)
159	57	M	AA	ABC/DTG/3TC	<50	77	77
430	60	M	AA	ABC/3TC, EFV	<50	184	140
PH029	45	M	AA	ABC/DTG/3TC	<50	33	31
1001	50	M	AA	FTC/ RPV/TAF	<20	81	75
1002	47	M	AA	FTC/RPV/TDF	<20	282	51
1003	60	M	AA	BIC/TAF/FTC	<20	290	53
1004	59	M	AA	EVG/COBI/FTC/TAF	<20	222	119
1005	52	M	AA	ABC/DTG/3TC	<20	102	43
1006	54	F	AA	DRV, RTV, RAL	<20	384	72
1007	62	M	AA	FTC/RPV/TDF	<20	234	10
1008	64	M	AA	DTG/FTC/TAF	29.6	354	58
1009	57	M	AA	ABC/DTG/3TC	<20	230	89
1010	53	F	AA	ABC/DTG/3TC	<20	198	38
1011	56	F	AA	EFV/FTC/TDF	<20	62	18
1015	55	M	W	DRV/COBI, DTG/RPV	<20	386	19
1017	58	M	W	ABC/3TC, RAL, LPV/r	<20	410	16
1019	54	F	AA	ABC/DTG/3TC	<20	156	21
1021	68	M	AA	ABC/3TC, ATV	<20	194	21
1024	38	M	W	FTC/RPV/TAF	<20	88	75
1025	47	M	W	FTC/RPV/TAF	<20	68	57
1026	68	M	AA	FTC/TDF, RAL	<20	292	77
1035	67	F	AA	EFV/FTC/TDF	39.9	326	83
1036	62	F	AA	EFV/FTC/TDF	<20	158	85
1037	59	M	AA	ABC/DTG/3TC	<20	254	43
1039	54	M	H	ABC/DTG/3TC	<20	149	28
1049	53	F	W	BIC/TAF/FTC	<20	169	165
1053	62	M	AA	BIC/TAF/FTC	<20	328	310
UCSF2006	68	M	W	ABC/DTG/3TC	<40	253	238
UCSF2147	62	M	Asian	BIC/FTC/TAF	<40	246	172

AA, African American; H, Hispanic; W, White/Caucasian

3TC, lamivudine; ABC, abacavir; ATV, atazanavir sulfate; BIC, bictegravir; COBI, cobicistat; DRV, darunavir ethanolate; DTG, dolutegravir; EVG, elvitegravir; FTC, emtricitabine; LPV, lopinavir; LPV/r, lopinavir/ritonavir; RAL, raltegravir; RPV, rilpivirine; RTV, ritonavir; TAF, tenofovir alefenamide; TDF, tenofovir disoproxil fumarate